Yu Zheng
Wen-Han Qian

Robotics Institute
Shanghai Jiao Tong University
Shanghai, China 200030
yuzheng007@sjtu.edu.cn
whqian@sh163.net

Coping with the Grasping Uncertainties in Force-closure Analysis

Abstract

Friction uncertainty and contact position uncertainty may have a disastrous effect on the closure properties of grasps. This paper reflects our approach to handling these uncertainties in force-closure analysis. The former uncertainty is measured by the possible reduction rate κ of friction coefficients, while the radius ρ of contact regions is used to quantify the latter uncertainty. The actual contact point may deviate from the desired position but not farther than $\rho \cdot \rho^S$, the supremum of ρ without loss of force-closure, indicates the grasp tolerance to contact position uncertainty. For investigating the above uncertainties systematically, we propose three new problems in force-closure: whether a grasp with given κ and ρ achieves force-closure, what value ρ^S equals if κ is given, and how ρ^S varies versus κ. To facilitate their solutions, we extend the scope of the infinitesimal motion approach from form-closure analysis to force-closure. A necessary and sufficient condition for force-closure is deduced by means of the duality between some convex cones, which play the key role in solving the problems. Finally, efficient algorithms are developed and applied to two illustrative examples.

KEY WORDS—duality, force-closure, grasping uncertainty, infinitesimal motion approach, multifingered robot hand

1. Introduction

During the past two decades, closure properties, including form-closure and force-closure, have been extensively studied in robotic grasping. Traditionally, a grasp is said to be form-closure if the object in any motion collides with the contacts, while a grasp is said to be force-closure if the contact forces can equilibrate any external wrench.

Form-closure is related only to the object geometry and the contact positions. It can be considered as a pure geometric property (Bicchi 1995). On the other hand, form-closure and force-closure are dual to each other (Nguyen 1988). If contacts are frictionless, force-closure has the same mathematical model as form-closure (Lakshminarayana 1978). Thus, in this paper, form-closure is included in force-closure as a special (frictionless) case.

The International Journal of Robotics Research
Vol. 24, No. 4, April 2004, pp. 311-327,
DOI: 10.1177/0278364905049469

1.1. Related Work on the Closure Properties

In this section, let us review previous research on the closure properties. There are several primary categories.

1.1.1. Required Number of Contacts

The number of contacts necessary for force-closure is a fundamental topic, which dates from the 19th century. Reuleaux (1875), who originally studied form-closure of mechanisms, indicated that four contacts are necessary to achieve a two-dimensional (2D) form-closure grasp. Subsequently, Somov (1900) found that seven contacts are needed in the three-dimensional (3D) case. Lakshminarayana (1978) reported the results. Mishra, Schwarz, and Sharir (1987) provided an upper bound of the number of contacts necessary to synthesize form-closure grasps on arbitrary objects. Markenscoff, Ni, and Papadimitriou (1990) proved that four/seven contacts are sufficient to achieve a form-closure grasp of a 2D/3D object without rotational symmetry, respectively. Also, three/four contacts are sufficient for any 2D/3D object with friction. Murray, Li, and Sastry (1994) summarized the number of contacts required for various contact models to grasp an object. Bicchi (1995) generalized the Reuleaux–Somoff condition, i.e., $m+1$ contacts are required to partially form-restrain an object with respect to an m-dimensional subspace.

1.1.2. Grasping Quality Evaluation

Li and Sastry (1988) presented three quality measures: the smallest singular value and the volume of the grasp matrix as well as a task-oriented measure. Trinkle (1992) produced a

quantitative measure of how far a grasp is from form-closure. Buss, Hashimoto, and Moore (1996) transformed the nonlinear friction constraints into positive definiteness constraints on a symmetric matrix, whose smallest eigenvalue was taken as a measure of the grasp stability margin. Zuo and Qian (1998) also proposed a quantitative index, which denotes the extent of a grasp to comply with the friction constraints. In terms of Q distance, Zhu and Wang (2003) quantified the capability of a grasp to equilibrate external wrenches. Other quality measures have been made by Abel, Holzmann, and McCarthy (1985), Barber et al. (1987), Ferrari and Canny (1992), Park and Starr (1992), Bekey et al. (1993), Mirtich and Canny (1994), Varma and Tasch (1995), and Zhang et al. (1997). Some quality measures can be applied to planning optimal grasps (e.g., Ferrari and Canny 1992; Zhu and Wang 2003).

1.1.3. Force-closure Conditions and Tests

There have been many conditions and testing methods for force-closure. We classify them into two schools.

The first school investigates force-closure in the wrench space. It began with the condition that the primitive contact wrenches positively span the entire wrench space (Salisbury and Roth 1983). This condition is equivalent to the situation that the origin of the wrench space is strictly inside the convex hull of the primitive contact wrenches (Mishra, Schwarz, and Sharir 1987). Without linearization of the friction cone, Li and Sastry (1988) asserted that a grasp is force-closure if and only if the origin of the wrench space is an interior point of the image of the grasp matrix with respect to the force domain. These statements imply that a grasp is force-closure if and only if it can generate resultant wrenches to constitute a convex hull containing the origin of the wrench space as an interior point. Nakamura, Nagai, and Yoshikawa (1989) adopted six linearly independent resultant wrenches and their opposites as vertices of such a convex hull. In fact, only seven resultant wrenches are enough as long as their convex hull is an origin-centered simplex in the wrench space. Based on these conditions, several algorithms for the force-closure test have been developed. Chen and Burdick (1993a) put forward a qualitative force-closure test for 2D n-finger grasps. To determine if the origin lies strictly inside the convex hull, Liu (1999) proposed a ray-shooting based algorithm, while Zhu and Wang (2003) presented an algorithm by computing the Q distance between the origin and the convex hull.

The second school studies force-closure in the contact force space, and it is led by the condition that the grasp matrix is surjective and that there is a strictly internal force (Murray, Li, and Sastry 1994). Various forms of this condition have appeared in the literature (Bicchi 1995; Chen, Walker, and Cheatham 1995; Buss, Hashimoto, and Moore 1996; Yoshikawa 1996; Zuo and Qian 1998; Han, Trinkle, and Li 2000). Bicchi (1995) and Yoshikawa (1996) took the kinematics of the grasping mechanism into account. Zuo and Qian (1998) extended the condition to soft multifingered grasps. Based on the result by Buss, Hashimoto, and Moore (1996), Han, Trinkle, and Li (2000) further cast the friction constraints into linear matrix inequalities and formulated the force-closure problem as a convex optimization problem involving linear matrix inequalities. For grasps with specific contact number and type, the force-closure condition was discussed in more detail (e.g., Nguyen 1986, 1988; Ponce, Stam, and Faverjon 1993; Ponce and Faverjon 1995; Ponce et al. 1997; Liu 2000; Li, Liu, and Cai 2003).

The first school's conditions require that the convex hull of the primitive contact wrenches be six-dimensional and the origin of the wrench space be in its relative interior. The existence of strictly internal forces is a necessary and sufficient condition for the origin being a relative interior point of the convex hull. On this basis, if the grasp matrix is surjective, the convex hull is six-dimensional and the origin lies in its interior. In addition, the surjection of the grasp matrix is a necessary condition for the convex hull being six-dimensional. Hence, the conditions of the two schools are equivalent. For frictionless grasps, they are of the same mathematical model (e.g., Trinkle 1992; Murray, Li, and Sastry 1994).

1.1.4. Force-closure Grasp Planning

In the beginning, the grasp planning focused on the grasps whose contact number and type are determined. Nguyen (1986, 1988) computed independent regions for two frictional and for four frictionless contacts to achieve force-closure grasps on polygons. Markenscoff and Papadimitriou (1989) proposed an analytic method for calculating the optimum grip of polygonal objects. Park and Starr (1992) synthesized three-fingered grasps on polygonal objects. Chen and Burdick (1993b) considered two-fingered antipodal point grasps of irregular 2D and 3D objects. Ponce and his colleagues (1993, 1995, 1997) extended Nguyen's idea to two-finger, three-finger and four-finger force-closure grasps on 2D curved, polygonal, and polyhedral objects, respectively. Tung and Kak (1996) brought forward an algorithm for synthesizing two-fingered force-closure grasps on polygons.

In recent years, planning algorithms have been oriented to grasps with arbitrary contact number. Liu (2000) presented an algorithm for computing n-finger grasps on polygons. Ding, Liu, and Wang (2001) considered 3D n-finger force-closure grasps where k fingers have been located in advance. With the ray-shooting based algorithm (Liu 1999), Ding et al. (2001) developed an algorithm for automatic selection of fixturing surfaces and points on polyhedral workpieces. By minimizing the Q distance, Zhu and Wang (2003) presented an algorithm for optimal grasp planning on 3D objects with curved surfaces.

1.2. Summary of Our Work

Previously, only a few papers have paid attention to the uncertainties in robotic grasping. Nakamura, Nagai, and Yoshikawa

(1989) mentioned friction uncertainty. Pai and Leu (1991) have computed the end-effector uncertainty resulting from the robot and have shown that the total uncertainty is the Minkowshi difference of the end-effector uncertainty and the task position uncertainty. Cheah et al. (1998) considered a grasping control for multifingered robot hands with uncertain Jacobian matrices. Schlegl and Buss (1998) compensated contact point position errors by the internal impedance. Up to now, no one has regarded the influence of uncertainties on the closure properties. In practice, however, some amount of uncertainty is inevitable and may cause a destructive effect.

This paper copes with grasping uncertainties in force-closure analysis. Force-closure is mainly threatened by friction uncertainty and contact position uncertainty. The former only occurs in the frictional case, while the latter usually occurs. We quantify these as the possible reduction rate κ of friction coefficients and the radius ρ of contact regions, respectively. The actual contact point may fall in the region R of the object surface contained in a closed ball of radius ρ centered at the desired contact point. ρ^S, the supremum of ρ without loss of force-closure, indicates the grasp tolerance to contact position uncertainty. Whether a grasp with given κ and ρ achieves force-closure, what value ρ^S equals if κ is given, and how ρ^S varies versus κ are three new problems we are solving in this paper. Moreover, because the existing methods are unsuitable for the problems (this will be discussed at the beginning of Section 4), we deal with force-closure analysis using an infinitesimal motion approach, which was originally applied to form-closure only (Bicchi 1995; Qian, Qiao, and Tso 2001). A necessary and sufficient condition for force-closure is deduced from the duality between four convex cones (see Figures 5 and 6), which are closely related to the closure properties. Compared with the work of Bicchi (1995) on form-closure, our work covers not only frictionless point contact but also point contact with friction and soft finger contact. Thus, the result is general. Different from the methods of Salisbury and Roth (1983), Liu (1999), and Zhu and Wang (2003), ours does not linearize the friction cone. Until now, the linearization could not be applied to soft finger contact. Simpler than the approaches taken by Murray, Li, and Sastry (1994), Chen, Walker, and Cheatham (1995), Zuo and Qian (1998), Buss, Hashimoto, and Moore (1996), and Han, Trinkle, and Li (2000), our force-closure test need not compute the rank and the null space of the grasp matrix. Finally, efficient algorithms are developed and demonstrated with two numerical examples.

The rest of this paper is arranged as follows. In Section 2 we review basic knowledge about robotic grasping. In Section 3 we discuss the uncertainties in force-closure analysis and their quantification. Subsequently, new problems in force-closure are presented. In Section 4 we apply an infinitesimal motion approach to force-closure analysis and then propose a necessary and sufficient condition for force-closure. In Section 5, algorithms for solving the presented problems are developed.

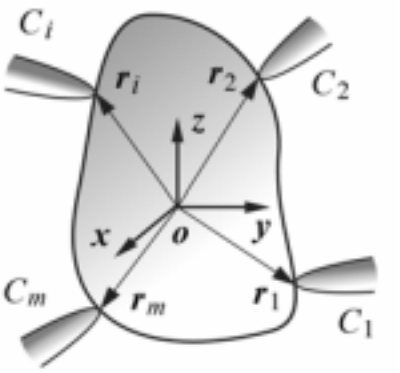

Fig. 1. An object grasped by a multifingered hand.

In Section 6 we implement the algorithms with two illustrative examples. A conclusion is made in Section 7 to highlight the key points. For use in Section 4, a method for computing the polar set of a compact convex set containing the origin as an interior point is addressed briefly in the Appendix.

2. Preliminaries

Consider an object grasped by a multifingered robot hand, as shown in Figure 1. Suppose that the grasp consists of m_0 frictionless point contacts (FPCs), m_f point contacts with friction (PCwFs), and m_s soft finger contacts (SFCs). The total number of contacts is

$$m = m_0 + m_f + m_s.$$

Figure 2 depicts the three common contact types.

The total contact force exerted upon the grasped object by the contacts can be written as

$$\boldsymbol{f} = \left[\boldsymbol{f}_1^{\mathrm{T}} \;\; \boldsymbol{f}_2^{\mathrm{T}} \;\; \cdots \;\; \boldsymbol{f}_m^{\mathrm{T}}\right]^{\mathrm{T}} \in \mathbb{R}^q \tag{1}$$

where $q = m_0 + 3m_f + 4m_s$ and $\boldsymbol{f}_i \in \mathbb{R}^{q_i}$ is the contact force at contact i ($i = 1, 2, \ldots, m$). For the three contact types, $\boldsymbol{f}_i$ and q_i are listed as follows:

$$\text{FPC: } \boldsymbol{f}_i = [f_{in}],\ q_i = 1$$

$$\text{PCwF: } \boldsymbol{f}_i = [f_{in} \;\; f_{io} \;\; f_{it}]^{\mathrm{T}},\ q_i = 3$$

$$\text{SFC: } \boldsymbol{f}_i = [f_{in} \;\; f_{io} \;\; f_{it} \;\; f_{is}]^{\mathrm{T}},\ q_i = 4$$

where f_{in} is the normal force, f_{io} and f_{it} are two tangential force components, and f_{is} is the spin moment about the contact normal.

The resultant wrench on the object can be calculated by

$$\boldsymbol{w} = \boldsymbol{G}\boldsymbol{f} \tag{2}$$

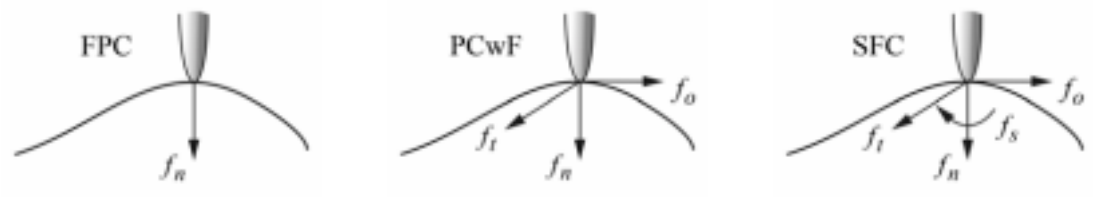

(a) (b) (c)

Fig. 2. Three common contact types: (a) frictionless point contact, at which the fingertip can exert only a normal force, (b) point contact with friction, at which the force exerted by the fingertip can be resolved into a normal force and two tangential force components, and (c) soft finger contact, at which the force exerted by the fingertip can be resolved into a normal force, two tangential force components and a spin moment about the contact normal.

where $\boldsymbol{w} \in \mathbb{R}^6$ is the resultant wrench and $\boldsymbol{G} = [\boldsymbol{G}_1\ \boldsymbol{G}_2\ \cdots\ \boldsymbol{G}_m] \in \mathbb{R}^{6\times q}$ is the grasp matrix. $\boldsymbol{G}_i \in \mathbb{R}^{6\times q_i}$ has one of the following forms determined by its contact type

$$\text{FPC:}\ \boldsymbol{G}_i = \begin{bmatrix} \boldsymbol{n}_i \\ \boldsymbol{r}_i \times \boldsymbol{n}_i \end{bmatrix} \tag{3}$$

$$\text{PCwF:}\ \boldsymbol{G}_i = \begin{bmatrix} \boldsymbol{n}_i & \boldsymbol{o}_i & \boldsymbol{t}_i \\ \boldsymbol{r}_i \times \boldsymbol{n}_i & \boldsymbol{r}_i \times \boldsymbol{o}_i & \boldsymbol{r}_i \times \boldsymbol{t}_i \end{bmatrix} \tag{4}$$

$$\text{SFC:}\ \boldsymbol{G}_i = \begin{bmatrix} \boldsymbol{n}_i & \boldsymbol{o}_i & \boldsymbol{t}_i & \boldsymbol{0} \\ \boldsymbol{r}_i \times \boldsymbol{n}_i & \boldsymbol{r}_i \times \boldsymbol{o}_i & \boldsymbol{r}_i \times \boldsymbol{t}_i & \boldsymbol{n}_i \end{bmatrix} \tag{5}$$

where $\boldsymbol{r}_i = [x_i\ y_i\ z_i]^{\mathrm{T}}$ is the position vector of contact i, $\boldsymbol{n}_i$ is the unit inward normal at contact i, and $\boldsymbol{o}_i$ and $\boldsymbol{t}_i$ are two unit tangent vectors satisfying $\boldsymbol{n}_i = \boldsymbol{o}_i \times \boldsymbol{t}_i$. For SFC, the fingertip contacts the object on a small area, generally elliptic, and $\boldsymbol{r}_i$ means the position vector of the area center.

From now on, we represent a grasp by its grasp matrix.

Let $\boldsymbol{w}_{ext}$ denote the external wrench. For equilibrium,

$$\boldsymbol{w} = -\boldsymbol{w}_{ext}.$$

To avoid separation and slippage at contact, $\boldsymbol{f}$ must satisfy the following contact constraints

$$\text{FPC:}\ f_{in} \geqslant 0 \tag{6}$$

$$\text{PCwF:}\ f_{in} \geqslant 0,\ \sqrt{f_{io}^2 + f_{it}^2} \leqslant \mu_i f_{in} \tag{7}$$

$$\text{SFCl:}\ f_{in} \geqslant 0,\ \frac{\sqrt{f_{io}^2 + f_{it}^2}}{\mu_i} + \frac{|f_{is}|}{\mu_{si}} \leqslant f_{in} \tag{8}$$

$$\text{SFCe:}\ f_{in} \geqslant 0,\ \sqrt{\frac{f_{io}^2 + f_{it}^2}{\mu_i^2} + \frac{f_{is}^2}{\mu_{si}'^2}} \leqslant f_{in} \tag{9}$$

where μ_i is the coefficient of tangential friction at contact i, and μ_{si} and μ_{si}' are the coefficients of torsional friction for SFC with linear approximation (SFCl) and elliptic approximation (SFCe), respectively (Howe, Kao, and Cutkosky 1988).

DEFINITION 1. A contact force $\boldsymbol{f}_i$ is said to be feasible if it satisfies eqs. (6), (7), (8), or (9). Furthermore, a total contact force $\boldsymbol{f}$ is said to be feasible if every $\boldsymbol{f}_i$ is feasible.

DEFINITION 2. A resultant wrench $\boldsymbol{w}$ is said to be feasible if there is a feasible $\boldsymbol{f}$ such that $\boldsymbol{w} = \boldsymbol{G}\boldsymbol{f}$.

DEFINITION 3. A grasp $\boldsymbol{G}$ is said to be force-closure if for any $\boldsymbol{w}_{ext}$, there exists a feasible $\boldsymbol{w}$ such that $\boldsymbol{w} = -\boldsymbol{w}_{ext}$.

3. Grasping Uncertainties and New Problems

A key influence on force-closure is the presence of grasping uncertainties, which are inevitable in practice and can lead to unpredictable, probably undesirable, results. So far, however, no one has mentioned the influence, although a few papers have referred to grasping uncertainties (Nakamura, Nagai, and Yoshikawa 1989; Pai and Leu 1991; Cheah et al. 1998; Schlegl and Buss 1998). Most publications assume that all given data under discussion are certain. For secure application of a force-closure grasp, it is necessary to figure out the capability of the grasp to tolerate grasping uncertainties. In this section, we first elaborate the uncertainties that threaten the force-closure property. Then we raise some new force-closure problems regarding the uncertainties.

3.1. Uncertainties in Force-closure Analysis

The force-closure property of grasps depends on the contact types and positions. For PCwF and SFC, friction coefficients are uncertain. For any contact, contact position uncertainty always exists. Both uncertainties have a stochastic nature. Figure 3 shows how they influence force-closure.

3.1.1. Friction Uncertainty

Friction, including tangential friction and torsional friction, is very sensitive to the environment. Under vibration, or with oil or water on the contact surface, the coefficients are liable to diminish. This changes the contact constraints (6)–(9) and thus affects the force-closure property, as shown in Figure 3(b).

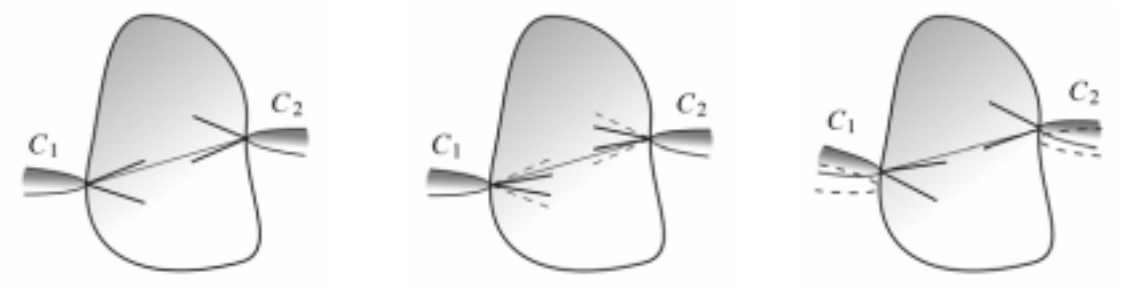

(a) (b) (c)

Fig. 3. A planar grasp with two point contacts with friction. (a) The grasp is force-closure, as the line connecting the contact points lies inside both friction cones. (b) Compared with (a), the grasp is not force-closure any more, owing to the decline of friction coefficients. The dashed lines depict the original friction cones. (c) Compared with (a), the grasp loses the force-closure property because of tiny deviations at the contact positions. The dashed curves indicate the original contact positions.

In order to deal with this uncertainty, we regard

$$\mu_i = \frac{1}{\kappa}\mu_{0i}, \quad \mu_{si} = \frac{1}{\kappa}\mu_{0si}, \quad \mu'_{si} = \frac{1}{\kappa}\mu'_{0si} \tag{10}$$

as the effective friction coefficients, where μ_{0i}, μ_{0si}, and μ'_{0si} are the nominal friction coefficients, and κ is the "possible reduction rate" ($\kappa \geqslant 1$).

It is assumed that all the friction coefficients decrease with the same rate κ. There are two reasons for this assumption. First, the friction coefficients depend on the contact surfaces (material, roughness, etc.), the substance between them (clean, dust, moisture, oil, or something else), and the environment (vibration, temperature, etc.). The uncertainties of these factors are often similar at all the contacts. Thus, it seems reasonable to assume a unique κ. Even if the possible reduction rates at different contacts are predicted to be unequal, we may take κ to be their maximum value for insurance. Secondly, if we take different reduction rates for each friction coefficient, then the problems would be too complicated owing to too many parameters. As a result, the tolerance of a grasp to the two uncertainties, for instance, cannot be clearly depicted by a 2D curve (see Figures 10 and 13).

3.1.2. Contact Position Uncertainty

Often contacts cannot be located exactly in the desired positions and obtaining their actual positions without uncertainty is very difficult, even impossible. Contact position uncertainty can be easily expressed by a position deviation, which occurs initially when the contact is located and further rises under the influence of the environment, such as vibration and shock. Additionally, in the case of rolling contact, the contact points are usually changing and uncertain during grasping. The position deviation alters the grasp matrices (3)–(5), so that the feasible resultant wrenches that the grasp can generate according to eq. (2) are transformed. The deviation may grow to such an extent that computation of force-closure grasps using exact contact positions may be completely unreliable in reality, as described in Figure 3(c).

To cope with this uncertainty, we allow the contact position $\boldsymbol{r}_i$ to be random on the object surface S in a region R_i bounded by a closed ball of radius ρ centered at the desired contact position $\boldsymbol{r}_{0i}$. The contact regions can be formulated as

$$R_i = \{\boldsymbol{r}_i \in S | \ \|\boldsymbol{r}_i - \boldsymbol{r}_{0i}\| \leqslant \rho\}, \quad i = 1, 2, \ldots, m. \tag{11}$$

Note that ρ must be bounded so that all the points in R_i are regular, because $\boldsymbol{n}_i, \boldsymbol{o}_i$, and $\boldsymbol{t}_i$ cannot be determined at singular points and then $\boldsymbol{G}$ cannot be written as eqs. (3)–(5). Let $\boldsymbol{G}_0$ denote the desired grasp that makes contact with the object at $\boldsymbol{r}_{0i}$, $i = 1, 2, \ldots, m$. Let ρ^S be the supremum of ρ such that the grasp keeps force-closure.

3.2. Problem Statement

PROBLEM 1. Suppose that a grasp $\boldsymbol{G}_0$, a radius ρ, nominal friction coefficients μ_{0i}, μ_{0si}, and μ'_{0si}, and a possible reduction rate κ are given. Determine whether the grasp $\boldsymbol{G}_0$ is force-closure or not.

PROBLEM 2. Suppose that a grasp $\boldsymbol{G}_0$, nominal friction coefficients μ_{0i}, μ_{0si}, and μ'_{0si}, and a possible reduction rate κ are given. Compute ρ^S.

PROBLEM 3. Suppose that a grasp $\boldsymbol{G}_0$ and nominal friction coefficients μ_{0i}, μ_{0si}, and μ'_{0si} are given. Draw the $\rho^S - \kappa$ curve.

The above problems are defined progressively. Problem 1 is natural and fundamental (both κ and ρ are constant). Problem 2 is to evaluate the grasp tolerance to contact position uncertainty under a given κ (κ is constant, while ρ^S is an

unknown to be determined). Problem 3 seeks the overall tolerance of a grasp to the two uncertainties by the $\rho^S - \kappa$ curve (both κ and ρ^S are variables).

4. An Infinitesimal Motion Approach to Force-closure Analysis

When trying to solve problems 1–3 with the existing methods of force-closure analysis, we have encountered some difficulties.

Based on linearization of the friction cone, the methods of the first school (see Section 1.1.3) could not be applied to SFC until now. Furthermore, the Q distance (Zhu and Wang 2003) is not so convenient to compute.

The methods of the second school (see Section 1.1.3) need to compute the rank and the null space of the grasp matrix $\boldsymbol{G}$. This is a tough task involving expensive computation cost, since in our problems $\boldsymbol{G}$ is varying in the contact regions R_i, $i = 1, 2, \ldots, m$. It is not worth searching R_i, $i = 1, 2, \ldots, m$ for the minimal rank of $\boldsymbol{G}$. The computed minimal rank is trustless, because a minimization algorithm may possibly meet with an ill-conditioned matrix that is sensitive to the round-off error in computing the rank. Instead of the rank of $\boldsymbol{G}$, the smallest non-zero singular value can be used to indicate how close $\boldsymbol{G}$ is to a matrix of lower rank, but the computation cost is increased. In addition, to check the existence of a strictly internal force subject to $\boldsymbol{r}_i \in R_i$, $i = 1, 2, \ldots, m$, a two-level optimization problem will be used. Thus, especially for multifingered grasps, the computational complexity is exorbitant.

The foregoing situation simulates us to explore a novel way. Inspired by the work of Bicchi (1995) on form-closure, we analyze the force-closure property from infinitesimal motions of the grasped object, rather than resultant wrenches or contact forces as usual. In order to bridge the gap between form-closure and force-closure, we investigate the relationship between several convex cones regarding infinitesimal motions and their dual cones concerning contact forces. By means of their duality, we obtain a new force-closure condition, which shows superior competence for solving problems 1–3.

4.1. Infinitesimal Motion of a Rigid Object

An infinitesimal motion $\boldsymbol{u} \in \mathbb{R}^6$ of a rigid object consists of an infinitesimal translation $\boldsymbol{\varepsilon} \in \mathbb{R}^3$ and an infinitesimal rotation $\boldsymbol{\varphi} \in \mathbb{R}^3$. This may cause the relative movement of the object to the fingertip at the contact point/area (see Figure 4).

For FPC and PCwF, the relative movement is just the translation of the object relative to the fingertip at the contact point $\boldsymbol{r}_i$, which can be characterized by

$$\boldsymbol{\delta}_i = \boldsymbol{\varepsilon} + \boldsymbol{\varphi} \times \boldsymbol{r}_i. \tag{12}$$

For SFC, different from point contact, the fingertip contacts the object on an area. Then the relative movement involves not only the translation but also the rotation of the object relative to the fingertip at the contact area, which are characterized by $\boldsymbol{\delta}_i$ and $\boldsymbol{\varphi}$, respectively.

Let d_{in}, d_{io}, and d_{it} be the components of $\boldsymbol{\delta}_i$ along $\boldsymbol{n}_i$, $\boldsymbol{o}_i$, and $\boldsymbol{t}_i$, respectively, and let d_{is} be the component of $\boldsymbol{\varphi}$ along $\boldsymbol{n}_i$, i.e.,

$$d_{in} = \boldsymbol{n}_i^{\mathrm{T}}\boldsymbol{\delta}_i, \quad d_{io} = \boldsymbol{o}_i^{\mathrm{T}}\boldsymbol{\delta}_i, \quad d_{it} = \boldsymbol{t}_i^{\mathrm{T}}\boldsymbol{\delta}_i, \quad d_{is} = \boldsymbol{n}_i^{\mathrm{T}}\boldsymbol{\varphi}. \tag{13}$$

The relative movement at $\boldsymbol{r}_i$ is consistent with the contact constraint if

$$\begin{aligned} \text{FPC:}\ & f_{in}d_{in} \geqslant 0 \\ \text{PCwF:}\ & f_{in}d_{in} + f_{io}d_{io} + f_{it}d_{it} \geqslant 0 \\ \text{SFC:}\ & f_{in}d_{in} + f_{io}d_{io} + f_{it}d_{it} + f_{is}d_{is} \geqslant 0 \end{aligned}$$

for all feasible $\boldsymbol{f}_i$. It is worth noting that only d_{in} has an effect on FPC, d_{in}, d_{io}, and d_{it} make sense together at PCwF, and all these components should be considered for SFC. The components of $\boldsymbol{\varphi}$ along $\boldsymbol{o}_i$ and $\boldsymbol{t}_i$ do not have any physical meaning for the three contact types (see Figure 4), since they have no counterparts in $\boldsymbol{f}_i$.

From eqs. (12) and (13), we can formulate a matrix equation similar to eq. (2)

$$\boldsymbol{d} = \boldsymbol{G}^{\mathrm{T}}\boldsymbol{u} \tag{14}$$

where $\boldsymbol{u} = \begin{bmatrix}\boldsymbol{\varepsilon}^{\mathrm{T}} & \boldsymbol{\varphi}^{\mathrm{T}}\end{bmatrix}^{\mathrm{T}} \in \mathbb{R}^6$, $\boldsymbol{d} = \begin{bmatrix}\boldsymbol{d}_1^{\mathrm{T}} & \boldsymbol{d}_2^{\mathrm{T}} & \cdots & \boldsymbol{d}_m^{\mathrm{T}}\end{bmatrix}^{\mathrm{T}} \in \mathbb{R}^q$, and $\boldsymbol{d}_i \in \mathbb{R}^{q_i}$ has one of the following forms:

$$\begin{aligned} \text{FPC:}\ & \boldsymbol{d}_i = [d_{in}] \\ \text{PCwF:}\ & \boldsymbol{d}_i = [d_{in} \ \ d_{io} \ \ d_{it}]^{\mathrm{T}} \\ \text{SFC:}\ & \boldsymbol{d}_i = [d_{in} \ \ d_{io} \ \ d_{it} \ \ d_{is}]^{\mathrm{T}}. \end{aligned}$$

$\boldsymbol{d}_i$ is called the functional movement, since only it makes sense in determining the consistency of the relative movement at $\boldsymbol{r}_i$. Accordingly, $\boldsymbol{d}$ is called the total functional movement.

DEFINITION 4. An infinitesimal motion $\boldsymbol{u}$ is said to be consistent (with the grasp) if $\boldsymbol{w}^{\mathrm{T}}\boldsymbol{u} \geqslant 0$ for all feasible $\boldsymbol{w}$.

DEFINITION 5. A functional movement $\boldsymbol{d}_i$ is said to be consistent (with fingertip i) if $\boldsymbol{f}_i^{\mathrm{T}}\boldsymbol{d}_i \geqslant 0$ for all feasible $\boldsymbol{f}_i$. Furthermore, a total functional movement $\boldsymbol{d}$ is said to be consistent if every $\boldsymbol{d}_i$ is consistent.

4.2. Convex Cones in Robotic Grasping

First, from Definition 1, the set of feasible total contact forces can be written as

$$\{\boldsymbol{f}\} = \{\boldsymbol{f} \in \mathbb{R}^q |\ \boldsymbol{f}_i \in \{\boldsymbol{f}_i\},\ i = 1, 2, \ldots, m\} \tag{15}$$

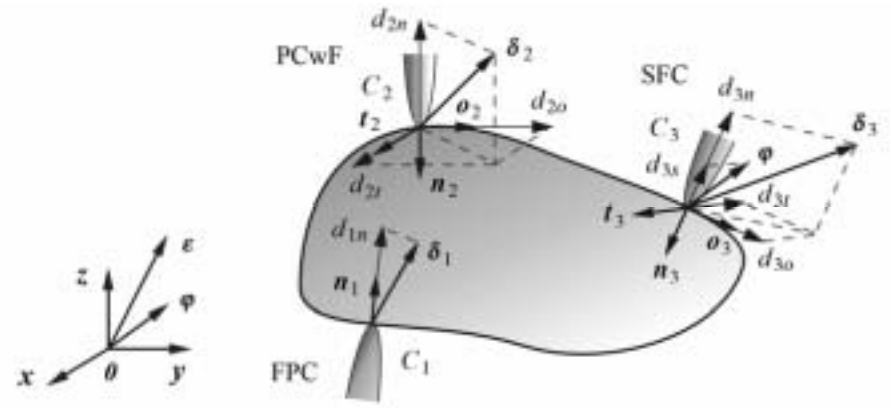

Fig. 4. Functional movements at three common contact types. Referring to Figure 2, the functional movement is corresponding to the contact force. At FPC (C_1), only the component d_{1n} of $\boldsymbol{\delta}_1$ along $\boldsymbol{n}_1$ makes sense. At PCwF (C_2), all the three components of $\boldsymbol{\delta}_2$ have physical meaning. At SFC (C_3), besides the components of $\boldsymbol{\delta}_3$, the component d_{3s} of $\boldsymbol{\varphi}$ along $\boldsymbol{n}_3$ cannot be neglected either.

where $\{\boldsymbol{f}_i\}$ is defined by

$$\text{FPC:}\quad \{\boldsymbol{f}_i\} = \{\boldsymbol{f}_i \in \mathbb{R} |\ f_{in} \geqslant 0\} \tag{16}$$

$$\text{PCwF:}\quad \{\boldsymbol{f}_i\} = \left\{\boldsymbol{f}_i \in \mathbb{R}^3 \middle|\ f_{in} \geqslant 0,\ \sqrt{f_{io}^2 + f_{it}^2} \leqslant \mu_i f_{in}\right\} \tag{17}$$

$$\text{SFCl:}\quad \{\boldsymbol{f}_i\} = \left\{\boldsymbol{f}_i \in \mathbb{R}^4 \middle|\ f_{in} \geqslant 0,\ \frac{\sqrt{f_{io}^2 + f_{it}^2}}{\mu_i} + \frac{|f_{is}|}{\mu_{si}} \leqslant f_{in}\right\} \tag{18}$$

$$\text{SFCe:}\quad \{\boldsymbol{f}_i\} = \left\{\boldsymbol{f}_i \in \mathbb{R}^4 \middle|\ f_{in} \geqslant 0,\ \sqrt{\frac{f_{io}^2 + f_{it}^2}{\mu_i^2} + \frac{f_{is}^2}{\mu_{si}'^2}} \leqslant f_{in}\right\}. \tag{19}$$

PROPOSITION 1. $\{\boldsymbol{f}_i\}$ for $i = 1, 2, \ldots, m$ is a closed convex cone with its vertex at the origin of $\mathbb{R}^{q_i}$. Furthermore, $\{\boldsymbol{f}\}$ is a closed convex cone with its vertex at the origin of $\mathbb{R}^q$.

Proof. See Li and Sastry (1988). □

Secondly, from Definition 2 and eq. (15), the set of feasible resultant wrenches has the form

$$\{\boldsymbol{w}\} = \left\{\boldsymbol{w} \in \mathbb{R}^6 \middle|\ \boldsymbol{w} = \boldsymbol{G}\boldsymbol{f} \text{ for some } \boldsymbol{f} \in \{\boldsymbol{f}\}\right\}. \tag{20}$$

PROPOSITION 2. $\{\boldsymbol{w}\}$ is a convex cone with its vertex at the origin of $\mathbb{R}^6$.

Proof. The property can be readily derived from Proposition 1 and eq. (20). □

Thirdly, from Definition 4 and eq. (20), the set of consistent infinitesimal motions can be formulated as

$$\{\boldsymbol{u}\} = \left\{\boldsymbol{u} \in \mathbb{R}^6 \middle|\ \boldsymbol{w}^{\mathrm{T}}\boldsymbol{u} \geqslant 0 \text{ for all } \boldsymbol{w} \in \{\boldsymbol{w}\}\right\}. \tag{21}$$

Equation (21) represents a cone, known as the dual cone of $\{\boldsymbol{w}\}$.

PROPOSITION 3. $\{\boldsymbol{u}\}$ is a closed convex cone with its vertex at the origin of $\mathbb{R}^6$.

Proof. It is known from convex analysis that the dual cone is indeed a cone, always convex and closed. □

Fourthly, from Definition 5 and eqs. (16)–(19), the set of consistent total functional movements can be written as

$$\{\boldsymbol{d}\} = \{\boldsymbol{d} \in \mathbb{R}^q |\ \boldsymbol{d}_i \in \{\boldsymbol{d}_i\},\ i = 1, 2, \ldots, m\} \tag{22}$$

where

$$\{\boldsymbol{d}_i\} = \left\{\boldsymbol{d}_i \in \mathbb{R}^{q_i} |\ \boldsymbol{f}_i^{\mathrm{T}}\boldsymbol{d}_i \geqslant 0 \text{ for all } \boldsymbol{f}_i \in \{\boldsymbol{f}_i\}\right\}. \tag{23}$$

Equation (23) means $\{\boldsymbol{d}_i\}$ is the dual cone of $\{\boldsymbol{f}_i\}$.

PROPOSITION 4. The following statements are true.

1. $\{\boldsymbol{d}_i\}$ for $i = 1, 2, \ldots, m$ is a closed convex cone with its vertex at the origin of $\mathbb{R}^{q_i}$. Furthermore, $\{\boldsymbol{d}\}$ is a closed convex cone with its vertex at the origin of $\mathbb{R}^q$.
2. $\{\boldsymbol{d}\}$ is the dual cone of $\{\boldsymbol{f}\}$:

$$\{\boldsymbol{d}\} = \left\{\boldsymbol{d} \in \mathbb{R}^q |\ \boldsymbol{f}^{\mathrm{T}}\boldsymbol{d} \geqslant 0 \text{ for all } \boldsymbol{f} \in \{\boldsymbol{f}\}\right\}. \tag{24}$$

Proof.

1. See the proof of Proposition 3.

2. We claim the equivalence of eqs. (22) and (24).

   Equation (22)⇒eq. (24): if $\boldsymbol{d}$ satisfies eq. (22), then from eq. (23), $\boldsymbol{f}_i^{\mathrm{T}}\boldsymbol{d}_i \geqslant 0$ for all $\boldsymbol{f}_i \in \{\boldsymbol{f}_i\}$, $i = 1, 2, \ldots, m$. Thus, $\boldsymbol{f}^{\mathrm{T}}\boldsymbol{d} = \sum_{i=1}^{m} \boldsymbol{f}_i^{\mathrm{T}}\boldsymbol{d}_i \geqslant 0$ for all $\boldsymbol{f} \in \{\boldsymbol{f}\}$, which means $\boldsymbol{d}$ satisfies eq. (24).

   Equation (24)⇒eq. (22): if $\boldsymbol{d}$ does not satisfy eq. (22), then from eq. (23), there is some $\boldsymbol{d}_i$ such that $\boldsymbol{f}_i^{\mathrm{T}}\boldsymbol{d}_i < 0$ for some $\boldsymbol{f}_i \in \{\boldsymbol{f}_i\}$. Thus, for some $\boldsymbol{f} = [\boldsymbol{0} \cdots \boldsymbol{f}_i^{\mathrm{T}} \cdots \boldsymbol{0}]^{\mathrm{T}} \in \{\boldsymbol{f}\}$, $\boldsymbol{f}^{\mathrm{T}}\boldsymbol{d} = \boldsymbol{f}_i^{\mathrm{T}}\boldsymbol{d}_i < 0$. This implies, if $\boldsymbol{d}$ satisfies eq. (24), it will also satisfy eq. (22). □

From the above, a necessary and sufficient condition for consistent infinitesimal motions can be derived below.

PROPOSITION 5. $\boldsymbol{u} \in \{\boldsymbol{u}\}$ if and only if $\boldsymbol{G}^{\mathrm{T}}\boldsymbol{u} \in \{\boldsymbol{d}\}$.

Proof. Sufficiency: if there exists $\boldsymbol{u} \in \mathbb{R}^6$ such that $\boldsymbol{G}^{\mathrm{T}}\boldsymbol{u} \in \{\boldsymbol{d}\}$, then from eq. (24), $\boldsymbol{f}^{\mathrm{T}}\boldsymbol{G}^{\mathrm{T}}\boldsymbol{u} \geqslant 0$ for all $\boldsymbol{f} \in \{\boldsymbol{f}\}$. According to eq. (20), this is equivalent to $\boldsymbol{w}^{\mathrm{T}}\boldsymbol{u} \geqslant 0$ for all $\boldsymbol{w} \in \{\boldsymbol{w}\}$. Thus $\boldsymbol{u} \in \{\boldsymbol{u}\}$ from eq. (21).

Necessity: if $\boldsymbol{u} \in \{\boldsymbol{u}\}$, then from eq. (21), $\boldsymbol{w}^{\mathrm{T}}\boldsymbol{u} \geqslant 0$ for all $\boldsymbol{w} \in \{\boldsymbol{w}\}$, which implies $\boldsymbol{f}^{\mathrm{T}}\boldsymbol{G}^{\mathrm{T}}\boldsymbol{u} \geqslant 0$ for all $\boldsymbol{f} \in \{\boldsymbol{f}\}$ by eq. (20). Hence, $\boldsymbol{G}^{\mathrm{T}}\boldsymbol{u} \in \{\boldsymbol{d}\}$ from eq. (24). □

4.3. Force-Closure Conditions

From Definition 3 and eq. (20), we have Theorem 1 directly.

THEOREM 1. A grasp is force-closure if and only if $\{\boldsymbol{w}\} = \mathbb{R}^6$.

THEOREM 2. A grasp is force-closure if and only if $\{\boldsymbol{u}\}$ consists only of the origin $\boldsymbol{0}$ of $\mathbb{R}^6$.

Proof. Sufficiency: when $\{\boldsymbol{u}\} = \{\boldsymbol{0} \in \mathbb{R}^6\}$, the dual cone of $\{\boldsymbol{u}\}$ is $\mathbb{R}^6$. Since $\{\boldsymbol{u}\}$ is the dual cone of $\{\boldsymbol{w}\}$ and $\{\boldsymbol{w}\}$ is convex, the dual cone of $\{\boldsymbol{u}\}$ is the closure of $\{\boldsymbol{w}\}$. Then the closure of $\{\boldsymbol{w}\}$ equals $\mathbb{R}^6$. Hence, $\{\boldsymbol{w}\} = \mathbb{R}^6$, which ensures that the grasp is force-closure by Theorem 1.

Necessity: from Theorem 1, the grasp being force-closure means $\{\boldsymbol{w}\} = \mathbb{R}^6$. Since $\{\boldsymbol{u}\}$ is the dual cone of $\{\boldsymbol{w}\}$, $\{\boldsymbol{u}\} = \{\boldsymbol{0} \in \mathbb{R}^6\}$ when $\{\boldsymbol{w}\} = \mathbb{R}^6$. □

Theorem 2 means that a force-closure grasp can prevent the object from moving. This is in accordance with our intuition.

THEOREM 3. A grasp is force-closure if and only if there does not exist non-zero $\boldsymbol{u} \in \mathbb{R}^6$ such that $\boldsymbol{G}^{\mathrm{T}}\boldsymbol{u} \in \{\boldsymbol{d}\}$.

Proof. Sufficiency: if there is not non-zero $\boldsymbol{u} \in \mathbb{R}^6$ such that $\boldsymbol{G}^{\mathrm{T}}\boldsymbol{u} \in \{\boldsymbol{d}\}$, then from Proposition 5, $\{\boldsymbol{u}\} = \{\boldsymbol{0} \in \mathbb{R}^6\}$. Therefore the grasp is force-closure from Theorem 2.

Necessity: if there is non-zero $\boldsymbol{u} \in \mathbb{R}^6$ such that $\boldsymbol{G}^{\mathrm{T}}\boldsymbol{u} \in \{\boldsymbol{d}\}$, then from Proposition 5, $\boldsymbol{u} \in \{\boldsymbol{u}\}$. Thus, the grasp is not force-closure from Theorem 2. □

Compared with the Bicchi (1995) form-closure condition, Theorem 3 involves all three contact types and is a general result. Different from the methods by Salisbury and Roth (1983), Liu (1999), and Zhu and Wang (2003), it does not employ linearization. Simpler than the methods by Murray, Li, and Sastry (1994), Chen, Walker, and Cheatham (1995), Zuo and Qian (1998), Buss, Hashimoto, and Moore (1996), and Han, Trinkle, and Li (2000), the force-closure test by Theorem 3 need not compute the rank and the null space of $\boldsymbol{G}$. If $\boldsymbol{G}$ is not full row rank, there exists non-zero $\boldsymbol{u}$ in the null space of $\boldsymbol{G}^{\mathrm{T}}$ such that $\boldsymbol{G}^{\mathrm{T}}\boldsymbol{u} = \boldsymbol{0} \in \{\boldsymbol{d}\}$; hence, the grasp $\boldsymbol{G}$ is not force-closure. Moreover, by Theorem 3, we can avoid solving problems 1–3 by two-level optimization (see Section 5).

4.4. Explicit Expression of $\{\boldsymbol{d}_i\}$

Although $\{\boldsymbol{d}_i\}$ is given by eq. (23) implicitly, we need to work out its explicit expression for applying Theorem 3 to problems 1–3.

The explicit expression of $\{\boldsymbol{d}_i\}$ is deduced in terms of the duality between $\{\boldsymbol{d}_i\}$ and $\{\boldsymbol{f}_i\}$, as indicated by eq. (23). Since $\{\boldsymbol{f}_i\}$ is a cone according to Proposition 1, it can be rewritten in the equivalent form:

$$\{\boldsymbol{f}_i\} = \left\{ \boldsymbol{f}_i = f_{in}[\,1\ \boldsymbol{x}_i^{\mathrm{T}}]^{\mathrm{T}} \in \mathbb{R}^{q_i} \,\middle|\, f_{in} \geqslant 0 \text{ and } \boldsymbol{x}_i \in \{\boldsymbol{x}_i\} \right\} \tag{25}$$

where $\{\boldsymbol{x}_i\}$ takes one of the following forms obtained by combining eqs. (16)–(19) and (25), respectively.

$$\text{FPC: } \{\boldsymbol{x}_i\} \text{ is a compact convex set of } \mathbb{R}^0 \text{ that contains the origin as an interior point} \tag{26}$$

$$\text{PCwF: } \{\boldsymbol{x}_i\} = \left\{ \boldsymbol{x}_i \in \mathbb{R}^2 \,\middle|\, \frac{1}{\mu_i}\sqrt{x_{i,1}^2 + x_{i,2}^2} \leqslant 1 \right\} \tag{27}$$

$$\text{SFCl: } \{\boldsymbol{x}_i\} = \left\{ \boldsymbol{x}_i \in \mathbb{R}^3 \,\middle|\, \frac{1}{\mu_i}\sqrt{x_{i,1}^2 + x_{i,2}^2} + \frac{1}{\mu_{si}}\left|x_{i,3}\right| \leqslant 1 \right\} \tag{28}$$

$$\text{SFCe: } \{\boldsymbol{x}_i\} = \left\{ \boldsymbol{x}_i \in \mathbb{R}^3 \,\middle|\, \sqrt{\frac{x_{i,1}^2 + x_{i,2}^2}{\mu_i^2} + \frac{x_{i,3}^2}{\mu_{si}'^2}} \leqslant 1 \right\} \tag{29}$$

where $x_{i,1}$, $x_{i,2}$, and $x_{i,3}$ are components of $\boldsymbol{x}_i$.

REMARK 1. For PCwF, SFCl, and SFCe, $\{\boldsymbol{x}_i\}$ is a compact convex set that contains the origin as an interior point. For unification, we assume that $\{\boldsymbol{x}_i\}$ for FPC is also such a set.

LEMMA 1. $\{\boldsymbol{d}_i\}$ can be rewritten in the equivalent form

$$\{\boldsymbol{d}_i\} = \left\{ \boldsymbol{d}_i = d_{in}[\,1\ \boldsymbol{y}_i^{\mathrm{T}}]^{\mathrm{T}} \in \mathbb{R}^{q_i} \,\middle|\, d_{in} \geqslant 0 \text{ and } \boldsymbol{y}_i \in \{\boldsymbol{y}_i\} \right\} \tag{30}$$

where $\{\boldsymbol{y}_i\}$ is the polar set of $\{\boldsymbol{x}_i\}$:

$$\{\boldsymbol{y}_i\} = \left\{ \boldsymbol{y}_i \in \mathbb{R}^{q_i - 1} \,\middle|\, \boldsymbol{x}_i^{\mathrm{T}}\boldsymbol{y}_i \leqslant 1 \text{ for all } \boldsymbol{x}_i \in \{\boldsymbol{x}_i\} \right\}. \tag{31}$$

Proof. We claim the equivalence of eqs. (23) and (30).

Equation (23)⇒eq. (30): let $\boldsymbol{d}_i = [\, d_{in}\ \boldsymbol{a}_i^{\mathrm{T}}]^{\mathrm{T}}$ where $\boldsymbol{a}_i \in \mathbb{R}^{q_i-1}$ and suppose $\boldsymbol{d}_i$ satisfies eq. (23). From eqs. (23) and (25) it follows that $\boldsymbol{f}_i^{\mathrm{T}}\boldsymbol{d}_i = f_{in}(d_{in} + \boldsymbol{x}_i^{\mathrm{T}}\boldsymbol{a}_i) \geqslant 0$ for all $\boldsymbol{f}_i \in \{\boldsymbol{f}_i\}$. From $\boldsymbol{f}_i \in \{\boldsymbol{f}_i\}$ when $f_{in} > 0$ and $\boldsymbol{x}_i = \boldsymbol{0}$, it next follows that $f_{in}d_{in} \geqslant 0$ for all $f_{in} > 0$. Thus $d_{in} \geqslant 0$.

If $d_{in} = 0$, then from eqs. (23) and (25), $\boldsymbol{f}_i^{\mathrm{T}}\boldsymbol{d}_i = f_{in}\boldsymbol{x}_i^{\mathrm{T}}\boldsymbol{a}_i \geqslant 0$ for all $\boldsymbol{f}_i \in \{\boldsymbol{f}_i\}$. From $f_{in} > 0$ we see that $\boldsymbol{x}_i^{\mathrm{T}}\boldsymbol{a}_i \geqslant 0$ for all $\boldsymbol{x}_i \in \{\boldsymbol{x}_i\}$. Note that, from eqs. (26)–(29), $\boldsymbol{0}$ is an interior point of $\{\boldsymbol{x}_i\}$. Hence $\boldsymbol{a}_i = \boldsymbol{0}$, and $\boldsymbol{d}_i = \boldsymbol{0}$ satisfies eq. (30).

If $d_{in} > 0$, from eqs. (23) and (25), $\boldsymbol{f}_i^{\mathrm{T}}\boldsymbol{d}_i = f_{in}d_{in}(1 + \boldsymbol{x}_i^{\mathrm{T}}\boldsymbol{y}_i) \geqslant 0$ for all $\boldsymbol{f}_i \in \{\boldsymbol{f}_i\}$ where $\boldsymbol{y}_i = \boldsymbol{a}_i/d_{in}$. From $f_{in} > 0$ it follows that $\boldsymbol{x}_i^{\mathrm{T}}\boldsymbol{y}_i \geqslant -1$ for all $\boldsymbol{x}_i \in \{\boldsymbol{x}_i\}$. Since $\{\boldsymbol{x}_i\}$ is symmetric about the origin, $\boldsymbol{x}_i^{\mathrm{T}}\boldsymbol{y}_i \leqslant 1$ for all $\boldsymbol{x}_i \in \{\boldsymbol{x}_i\}$; that is, $\boldsymbol{y}_i \in \{\boldsymbol{y}_i\}$. Therefore, $\boldsymbol{d}_i$ satisfies eq. (30).

Equation (30)⇒eq. (23): suppose that $\boldsymbol{d}_i = d_{in}[\, 1\ \boldsymbol{y}_i^{\mathrm{T}}]^{\mathrm{T}}$ satisfies eq. (30). From eq. (31) and the symmetry of $\{\boldsymbol{x}_i\}$ it follows that $\boldsymbol{x}_i^{\mathrm{T}}\boldsymbol{y}_i \geqslant -1$ for all $\boldsymbol{x}_i \in \{\boldsymbol{x}_i\}$. From eqs. (25) and (30) it next follows that $\boldsymbol{f}_i^{\mathrm{T}}\boldsymbol{d}_i = f_{in}d_{in}(\boldsymbol{x}_i^{\mathrm{T}}\boldsymbol{y}_i + 1) \geqslant 0$ for all $\boldsymbol{f}_i \in \{\boldsymbol{f}_i\}$. Thus $\boldsymbol{d}_i$ satisfies eq. (23). □

The Appendix offers an approach to computing the polar set of a compact convex set containing the origin as an interior point. Using this approach, $\{\boldsymbol{y}_i\}$ for eqs. (26)–(29) is computed as follows.

$$\text{FPC: } \{\boldsymbol{y}_i\} \text{ is a compact convex set of } \mathbb{R}^0 \text{ that contains the origin as an interior point} \tag{32}$$

$$\text{PCwF: } \{\boldsymbol{y}_i\} = \left\{ \boldsymbol{y}_i \in \mathbb{R}^2 \middle|\ \mu_i\sqrt{y_{i,1}^2 + y_{i,2}^2} \leqslant 1 \right\} \tag{33}$$

$$\text{SFCl: } \{\boldsymbol{y}_i\} = \left\{ \boldsymbol{y}_i \in \mathbb{R}^3 \middle|\ \mu_i\sqrt{y_{i,1}^2 + y_{i,2}^2} \leqslant 1, \mu_{si}\left|y_{i,3}\right| \leqslant 1 \right\} \tag{34}$$

$$\text{SFCe: } \{\boldsymbol{y}_i\} = \left\{ \boldsymbol{y}_i \in \mathbb{R}^3 \middle|\ \sqrt{\mu_i^2(y_{i,1}^2 + y_{i,2}^2) + \mu_{si}'^2 y_{i,3}^2} \leqslant 1 \right\} \tag{35}$$

where $y_{i,1}$, $y_{i,2}$, and $y_{i,3}$ are components of $\boldsymbol{y}_i$.

Finally, substituting eqs. (32)–(35) into eq. (30) respectively yields

$$\text{FPC: } \{\boldsymbol{d}_i\} = \{\boldsymbol{d}_i \in \mathbb{R} |\ d_{in} \geqslant 0\} \tag{36}$$

$$\text{PCwF: } \{\boldsymbol{d}_i\} = \left\{ \boldsymbol{d}_i \in \mathbb{R}^3 \middle|\ \mu_i\sqrt{d_{io}^2 + d_{it}^2} \leqslant d_{in} \right\} \tag{37}$$

$$\text{SFCl: } \{\boldsymbol{d}_i\} = \left\{ \boldsymbol{d}_i \in \mathbb{R}^4 \middle|\ \mu_i\sqrt{d_{io}^2 + d_{it}^2} \leqslant d_{in}, \mu_{si}\left|d_{is}\right| \leqslant d_{in} \right\} \tag{38}$$

$$\text{SFCe: } \{\boldsymbol{d}_i\} = \left\{ \boldsymbol{d}_i \in \mathbb{R}^4 \middle|\ \sqrt{\mu_i^2(d_{io}^2 + d_{it}^2) + \mu_{si}'^2 d_{is}^2} \leqslant d_{in} \right\}. \tag{39}$$

Figure 5 depicts $\{\boldsymbol{f}_i\}$ and $\{\boldsymbol{d}_i\}$ for various contacts. The relationships between $\{\boldsymbol{x}_i\}$, $\{\boldsymbol{y}_i\}$, $\{\boldsymbol{f}_i\}$, $\{\boldsymbol{d}_i\}$, $\{\boldsymbol{f}\}$, $\{\boldsymbol{d}\}$, $\{\boldsymbol{w}\}$, and $\{\boldsymbol{u}\}$ are summarized in Figure 6.

5. Efficient Algorithms

Based on Theorem 3, we provide the algorithms to solve problems 1–3. Herein, we adopt SFCe, but the presented algorithms can also be applied to SFCl.

ALGORITHM 1. (solving problem 1). The algorithm searches the contact regions R_i, $i = 1, 2, \ldots, m$ for the contact positions such that the grasp is not force-closure.

Step 1. Let $\mu_i = \mu_{0i}/\kappa$ and $\mu_{si} = \mu_{0si}/\kappa$ for $i = 1, 2, \ldots, m$.

Step 2. Let $\boldsymbol{d} = \boldsymbol{G}^{\mathrm{T}}\boldsymbol{u}$. Set ζ_i for $i = 1, 2, \ldots, m$ as follows:

$$\text{FPC: } \zeta_i = d_{in}$$

$$\text{PCwF: } \zeta_i = d_{in} - \mu_i\sqrt{d_{io}^2 + d_{it}^2}$$

$$\text{SFCe: } \zeta_i = d_{in} - \sqrt{\mu_i^2(d_{io}^2 + d_{it}^2) + \mu_{si}'^2 d_{is}^2}.$$

Seek $\boldsymbol{u}^* \in \{\boldsymbol{u} |\ \|\boldsymbol{u}\| = 1\}$ and $\boldsymbol{r}_i^* \in R_i$, $i = 1, 2, \ldots, m$, for which $\zeta = \min\limits_{1 \leqslant i \leqslant m} \zeta_i$ is maximal. This can be formulated as

$$\begin{aligned} &\text{Maximize } \zeta = \min_{1 \leqslant i \leqslant m} \zeta_i \\ &\text{subject to } \|\boldsymbol{u}\| = 1,\ \boldsymbol{r}_i \in R_i,\ i = 1, 2, \ldots, m. \end{aligned} \tag{40}$$

Suppose that the maximal objective value of eq. (40) is ζ^*, which gives the results according to Theorem 3.

1. If $\zeta^* < 0$, then $\boldsymbol{G}^{\mathrm{T}}\boldsymbol{u} \notin \{\boldsymbol{d}\}$ for any $\boldsymbol{r}_i \in R_i$, $i = 1, 2, \ldots, m$, and non-zero $\boldsymbol{u} \in \mathbb{R}^6$. Thus the given grasp $\boldsymbol{G}_0$ is force-closure with κ and ρ.
2. If $\zeta^* \geqslant 0$, then $\boldsymbol{G}^{\mathrm{T}}\boldsymbol{u} \in \{\boldsymbol{d}\}$ for $\boldsymbol{r}_i^*$, $i = 1, 2, \ldots, m$, and $\boldsymbol{u}^*$. This means the grasp $\boldsymbol{G}^*$, whose contact positions are $\boldsymbol{r}_i^*$, $i = 1, 2, \ldots, m$, is a non-force-closure grasp and $\boldsymbol{u}^*$ is a consistent infinitesimal motion. Thus, the given grasp $\boldsymbol{G}_0$ is not force-closure with κ and ρ.

REMARK 2. ζ^* provides a the-less-the-better quality measure of the grasp $\boldsymbol{G}_0$ with respect to the given κ and ρ. The grasp $\boldsymbol{G}^*$ is the closest to non-force-closure ($\zeta^* < 0$) or the furthest from force-closure ($\zeta^* \geqslant 0$) within the contact regions. In addition, when $\kappa = 1$ and $\rho = 0$, the algorithm degenerates into a force-closure test for the grasp $\boldsymbol{G}_0$ disregarding the uncertainties.

When κ is fixed, ζ^* is continuous and monotonically increasing with respect to ρ on $[0, \rho^U]$, where ρ^U is the upper bound of ρ such that the points in R_i for $i = 1, 2, \ldots, m$ are all regular.

For a given κ, if $\zeta^*(0) < 0$ and $\zeta^*(\rho^U) \geqslant 0$, there is $\rho \in [0, \rho^U]$ such that $\zeta^*(\rho) = 0$. Then the minimum ρ satisfying $\zeta^*(\rho) = 0$ is the supremum of the radius we are looking

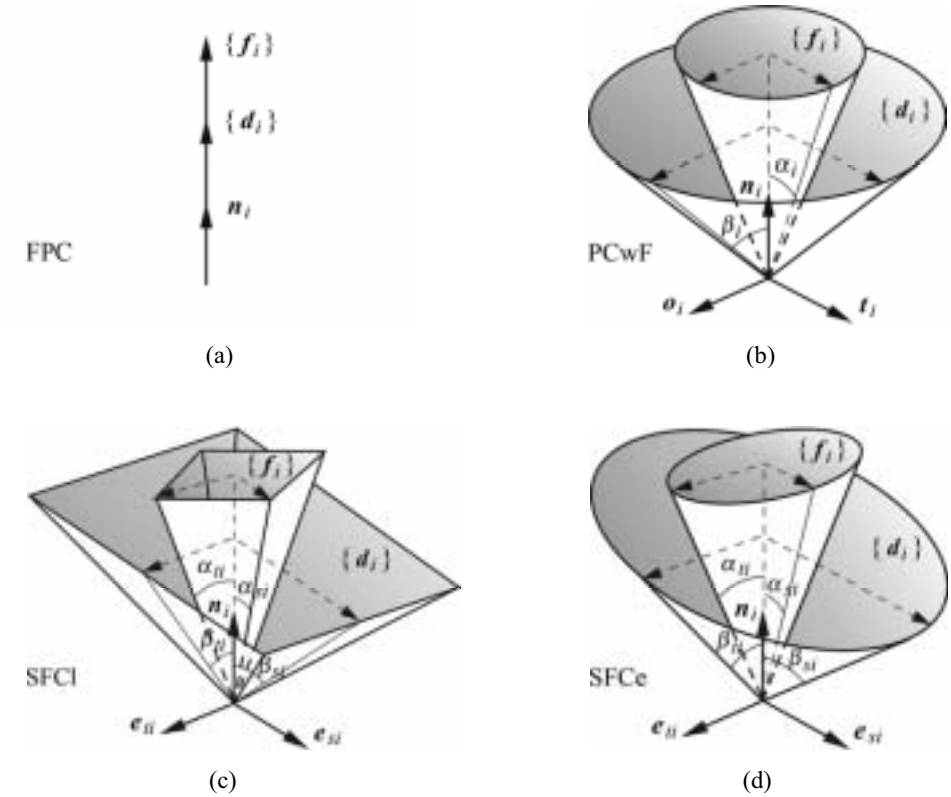

(a) (b)

(c) (d)

Fig. 5. Graphic representations of $\{\boldsymbol{f}_i\}$ and $\{\boldsymbol{d}_i\}$. The former denotes the feasible contact force set, while the latter denotes the consistent functional movement set dual to the former. Both sets are closed convex cones. (a) For FPC, $\{\boldsymbol{f}_i\}$ and $\{\boldsymbol{d}_i\}$ are half-lines along $\boldsymbol{n}_i$. (b) For PcwF, $\{\boldsymbol{f}_i\}$ and $\{\boldsymbol{d}_i\}$ are circular cones in the coordinate frame $[\boldsymbol{n}_i, \boldsymbol{o}_i, \boldsymbol{t}_i]$.$\alpha_i = \tan^{-1}\mu_i$ and $\beta_i = \tan^{-1}\mu_i^{-1}$. (c) For SFCl, in the coordinate frame $[\boldsymbol{n}_i, \boldsymbol{e}_{ti}, \boldsymbol{e}_{si}]$, $\{\boldsymbol{f}_i\}$ is a rhombic cone, whereas $\{\boldsymbol{d}_i\}$ is a rectangular cone. The coordinate of $\boldsymbol{f}_i$ with respect to $\boldsymbol{e}_{ti}$ is $\sqrt{f_{io}^2 + f_{it}^2}$ or $-\sqrt{f_{io}^2 + f_{it}^2}$, while that with respect to $\boldsymbol{e}_{si}$ is f_{is} or $-f_{is}$. $\alpha_{ti} = \tan^{-1}\mu_i$, $\alpha_{si} = \tan^{-1}\mu_{si}$, $\beta_{ti} = \tan^{-1}\mu_i^{-1}$, $\beta_{si} = \tan^{-1}\mu_{si}^{-1}$. (d) For SFCe, $\{\boldsymbol{f}_i\}$ and $\{\boldsymbol{d}_i\}$ are elliptic cones. $\alpha_{si} = \tan^{-1}\mu'_{si}$ and $\beta_{si} = \tan^{-1}\mu'^{-1}_{si}$.

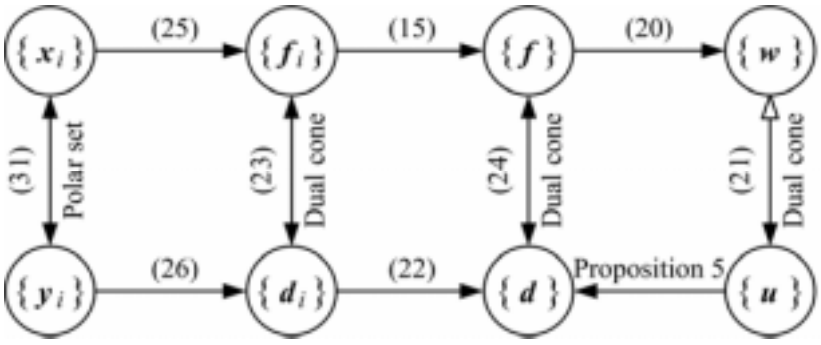

Fig. 6. Diagram of relationships. The hollow arrow represents that the dual cone of $\{\boldsymbol{u}\}$ is not $\{\boldsymbol{w}\}$ but the closure of $\{\boldsymbol{w}\}$ if $\{\boldsymbol{w}\}$ is not closed.

for in problem 2. Accordingly, problem 2 is formulated as an algebraic equation of one variable.

ALGORITHM 2. (solving problem 2). The algorithm computes the supremum ρ^S of the radius ρ within which the given grasp $\boldsymbol{G}_0$ is force-closure.

Step 1. Compute $\zeta^*(0)$ by Algorithm 1. If $\zeta^*(0) \geqslant 0$, then $\rho^S = 0$ and the algorithm ends; otherwise, go to Step 2.

Step 2. Determine the upper bound ρ^U of ρ. Compute $\zeta^*(\rho^U)$ by Algorithm 1. If $\zeta^*(\rho^U) < 0$, $\rho^S = \rho^U$ and the algorithm ends; otherwise, go to Step 3.

Step 3. Now, $\zeta^*(0) < 0$ and $\zeta^*(\rho^U) \geqslant 0$. We use the bisection method to search for the minimum solution to the equation $\zeta^*(\rho) = 0$ on $[0, \rho^U]$. Initialize $\rho_1 = 0$ and $\rho_2 = \rho^U$.

Step 4. $\rho = (\rho_1 + \rho_2)/2$. Compute $\zeta^*(\rho)$ by Algorithm 1. If $\zeta^*(\rho) < 0$, then $\rho_1 = \rho$; otherwise, $\rho_2 = \rho$.

Step 5. If $\rho_2 - \rho_1 \leqslant \varepsilon_\rho$ ($\varepsilon_\rho > 0$ is the termination tolerance on ρ), then $\rho^S = (\rho_1 + \rho_2)/2$ and the algorithm ends; otherwise, return to Step 4.

REMARK 3. ρ^S represents the capability of the grasp $\boldsymbol{G}_0$ to overcome contact position uncertainty with respect to κ. In steps 3–5, besides the bisection method, other numerical methods for solving algebraic equations can also be used.

Notice that ρ^S is related to κ, and obviously, ρ^S is monotonically decreasing on $\kappa \geqslant 1$. This implies that the grasp tolerances to the two grasping uncertainties are restricted by each other. Thus, we require Algorithm 3.

ALGORITHM 3. (solving problem 3). The algorithm plots the $\rho^S - \kappa$ curve to show the relation between ρ^S and κ. It is a straightforward application of Algorithm 2. We begin with $\kappa = 1$ and compute ρ^S at some intervals.

REMARK 4. The $\rho^S - \kappa$ curve offers a complete report on the closure properties of the grasp $\boldsymbol{G}_0$ and its capability to tolerate the two grasping uncertainties. If $\rho^S > 0$ at $\kappa = 1$, then the grasp $\boldsymbol{G}_0$ is force-closure; otherwise $\rho^S = 0$ and the grasp $\boldsymbol{G}_0$ is not force-closure. If $\lim_{\kappa \to +\infty} \rho^S(\kappa) = \text{Const} > 0$, then the grasp $\boldsymbol{G}_0$ is form-closure; otherwise $\lim_{\kappa \to +\infty} \rho^S(\kappa) = 0$ and the grasp $\boldsymbol{G}_0$ is not form-closure.

6. Numerical Examples

We implement the presented algorithms using the optimization toolbox of MATLAB on Pentium-IV PC.

EXAMPLE 1. Figure 7 depicts a wedge with vertices $V_1(25, 50\sqrt{3}, 0)$, $V_2(-25, 50\sqrt{3}, 0)$, $V_3(-25, 0, 50)$, $V_4(25, 0, 50)$, $V_5(25, 0, 0)$, $V_6(-25, 0, 0)$. It is grasped by a seven-fingered robot hand, whose fingertips make a SFC (C_1), two PCwFs (C_2, C_3), and four FPCs ($C_4 - C_7$). The nominal friction coefficients $\mu_0 = 0.2$ and $\mu_{s0} = 0.2$mm.

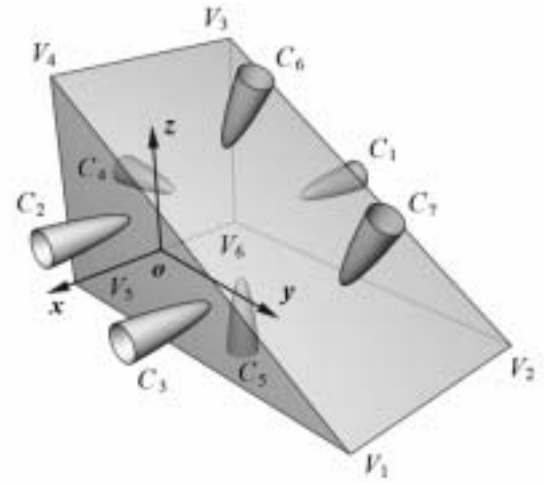

Fig. 7. A wedge is grasped by a seven-fingered gripper with a soft finger contact C_1, two point contacts with friction C_2 and C_3, and four frictionless point contacts C_4–C_7.

The desired contact positions are as follows:

$$\boldsymbol{r}_{01} = [-25\ 25\ 15]^{\mathrm{T}}, \quad \boldsymbol{r}_{02} = [25\ 25\ 25]^{\mathrm{T}},$$

$$\boldsymbol{r}_{03} = [25\ 50\ 15]^{\mathrm{T}}, \quad \boldsymbol{r}_{04} = [-5\ 0\ 15]^{\mathrm{T}},$$

$$\boldsymbol{r}_{05} = [-5\ 25\ 0]^{\mathrm{T}}, \quad \boldsymbol{r}_{06} = \left[0\ 15\sqrt{3}\ 35\right]^{\mathrm{T}},$$

$$\boldsymbol{r}_{07} = \left[0\ 35\sqrt{3}\ 15\right]^{\mathrm{T}}.$$

The contact regions can be formulated as

$$R_1 = \left\{\boldsymbol{r}_1 \middle|\ (r_{12} - 25)^2 + (r_{13} - 15)^2 \leqslant \rho^2,\ r_{11} = -25\right\},$$

$$R_2 = \left\{\boldsymbol{r}_2 \middle|\ (r_{22} - 25)^2 + (r_{23} - 25)^2 \leqslant \rho^2,\ r_{21} = 25\right\},$$

$$R_3 = \left\{\boldsymbol{r}_3 \middle|\ (r_{32} - 50)^2 + (r_{33} - 15)^2 \leqslant \rho^2,\ r_{31} = 25\right\},$$

$$R_4 = \left\{\boldsymbol{r}_4 \middle|\ (r_{41} + 5)^2 + (r_{43} - 15)^2 \leqslant \rho^2,\ r_{42} = 0\right\},$$

$$R_5 = \left\{\boldsymbol{r}_5 \middle|\ (r_{51} + 5)^2 + (r_{52} - 25)^2 \leqslant \rho^2,\ r_{53} = 0\right\},$$

$$R_i = \left\{\boldsymbol{r}_i \middle|\ \|\boldsymbol{r}_i - \boldsymbol{r}_{0i}\| \leqslant \rho,\ r_{i2} + \sqrt{3}\, r_{i3} = 50\sqrt{3}\right\}$$

for $i = 6, 7$.

First, using Algorithm 1 with $\kappa = 1$, we obtain the $\zeta^* - \rho$ (maximal objective value versus radius) curve, as shown in Figure 8. For $\rho = 0$ and $\rho = 4$, $\zeta^* = -6.1697 \times 10^{-2} < 0$ and $\zeta^* = 5.6618 \times 10^{-2} > 0$, respectively. This means that

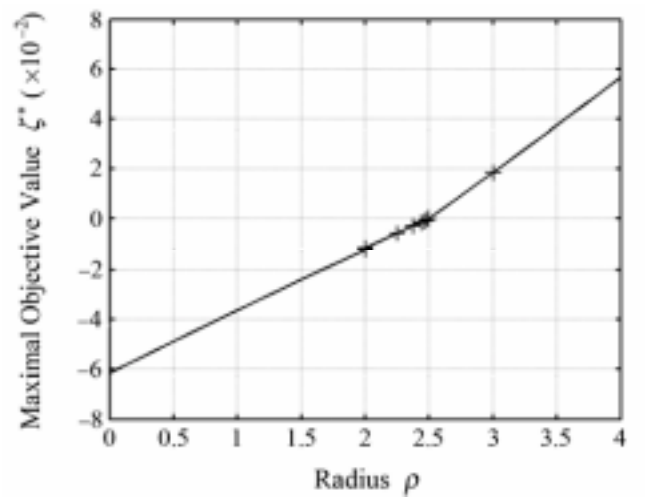

Fig. 8. The $\zeta^* - \rho$ curve obtained by Algorithm 1 when $\kappa = 1$. The plus signs indicate the data (ρ, ζ^*) in running Algorithm 2.

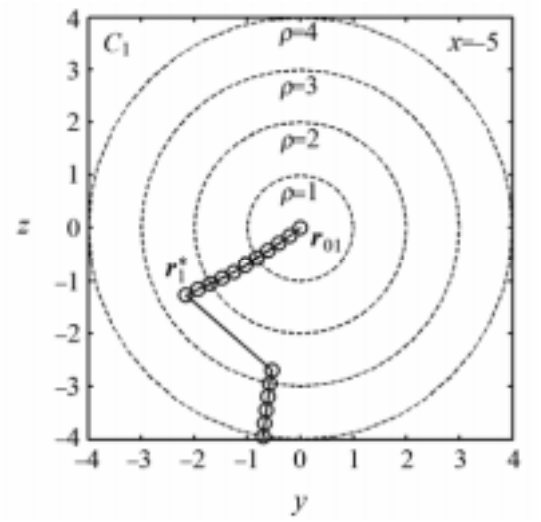

Fig. 9. The trajectory of r_1^*.

the grasp $\boldsymbol{G}_0$ is force-closure, but not force-closure with the radius $\rho = 4$, since we find a non-force-closure grasp within the contact regions as

$$\boldsymbol{r}_1^* = [-25.0000\ 24.2974\ 11.0622]^{\mathrm{T}},$$

$$\boldsymbol{r}_2^* = [25.0000\ 28.5222\ 23.1580]^{\mathrm{T}},$$

$$\boldsymbol{r}_3^* = [25.0000\ 50.7033\ 18.9377]^{\mathrm{T}},$$

$$\boldsymbol{r}_4^* = [-1.0000\ 0.0\ 15.0003]^{\mathrm{T}},$$

$$\boldsymbol{r}_5^* = [-1.0000\ 25.0002\ 0.0]^{\mathrm{T}},$$

$$\boldsymbol{r}_6^* = [-2.5999\ 25.9808\ 35.0000]^{\mathrm{T}},$$

$$\boldsymbol{r}_7^* = [-4.0000\ 60.6219\ 14.9999]^{\mathrm{T}}.$$

$\boldsymbol{u}^* = [9.9138\ 0.6496\ 1.0336\ 0.0\ -0.4674\ 0.0834]^{\mathrm{T}} \times 10^{-1}$ is a direction of consistent infinitesimal motions of the wedge at the moment. The required CPU time for running Algorithm 1 once is 1.02 s.

In Figure 8, the $\zeta^* - \rho$ curve seems to consist of two line segments with a slope change around $\rho = 2.5$. This is because $\boldsymbol{r}_i^*$ with respect to ρ traces a line turning suddenly around $\rho = 2.5$, as shown in Figure 9 which takes $\boldsymbol{r}_1^*$ as an example.

Next, taking $\rho^U = 4$ and $\varepsilon_\rho = 10^{-4}$, we apply Algorithm 2 to computing ρ^S of $\boldsymbol{G}_0$ with respect to $\kappa = 1$. The data in each loop are listed in Table 1, and $(\rho,\ \zeta^*)$ is marked by plus signs in Figure 8. The algorithm terminates at $\rho_1 = 2.4999$ and $\rho_2 = 2.5000$. In the end, $\rho^S = 2.5000$, for which $\zeta^* = -0.0002 \times 10^{-2}$. The required CPU time is 13.84 s.

Finally, Figure 10 shows the $\rho^S - \kappa$ curve obtained by Algorithm 3. As clearly reflected in Figure 10, ρ^S is monotonically decreasing on $\kappa \geqslant 1$. Since $\rho^S = 2.5000 > 0$ at $\kappa = 1$, the grasp $\boldsymbol{G}_0$ is force-closure. As κ increases, ρ^S approaches a positive number. Using Algorithm 1, we have $\left|\rho^S(\kappa) - 1.3175\right| < 10^{-4}$ for $\kappa > 10^4$. This means that $\boldsymbol{G}_0$ is not only force-closure but also form-closure; hence friction uncertainty can be entirely overcome.

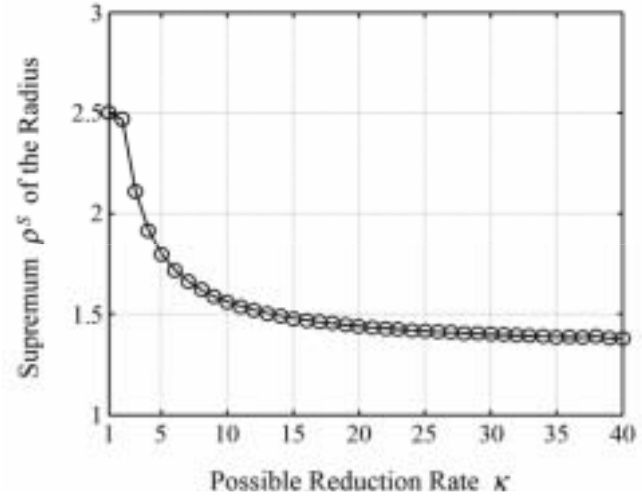

Fig. 10. The $\rho^S - \kappa$ curve for $\boldsymbol{G}_0$ obtained by Algorithm 3.

EXAMPLE 2. Figure 11 represents an L-shaped pipe grasped by a three-fingered robot hand. All the contacts $(C_1 - C_3)$ are PCwFs where the nominal friction coefficient $\mu_0 = 0.4$. The pipe can be expressed piecewise by

Table 1. Data During the Iteration by Bisection in Running Algorithm 2 for Example 1

Loop	ρ_1	ρ_2	$\rho = (\rho_1 + \rho_2)/2$	$\zeta^*(10^{-2})$
1	0	4	2.0000	–1.1853
2	2.0000	4	3.0000	1.8513
3	2.0000	3.0000	2.5000	0.0000
4	2.0000	2.5000	2.2500	–0.5891
5	2.2500	2.5000	2.3750	–0.2936
6	2.3750	2.5000	2.4375	–0.1466
7	2.4375	2.5000	2.4688	–0.0776
8	2.4688	2.5000	2.4844	–0.0387
9	2.8444	2.5000	2.4922	–0.0184
10	2.4922	2.5000	2.4961	–0.0092
11	2.4961	2.5000	2.4980	–0.0049
12	2.4980	2.5000	2.4990	–0.0024
13	2.4990	2.5000	2.4995	–0.0012
14	2.4995	2.5000	2.4998	–0.0006
15	2.4998	2.5000	2.4999	–0.0003

$$S_1\colon \begin{cases} r_{11} = 10\cos\phi_1 & 0 \leqslant \phi_1 < 2\pi \\ r_{12} = \varphi_1 & 0 \leqslant \varphi_1 \leqslant 40 \\ r_{13} = 10\sin\phi_1 + 40, & \end{cases}$$

$$S_2\colon \begin{cases} r_{21} = 10\sin\phi_2 & 0 \leqslant \phi_2 < 2\pi \\ r_{22} = (10\cos\varphi_2 + 40)\cos\varphi_2 & \pi/2 \leqslant \varphi_2 \leqslant \pi \\ r_{23} = (10\cos\varphi_2 + 40)\sin\varphi_2 & \end{cases}$$

$$S_3\colon \begin{cases} r_{31} = 10\cos\phi_3 & 0 \leqslant \phi_3 < 2\pi \\ r_{32} = 10\sin\phi_3 - 40 & -50 \leqslant \varphi_3 \leqslant 0 \\ r_{33} = \varphi_3 & \end{cases}$$

The desired contact positions are

$$\phi_{01} = \pi/2, \quad \varphi_{01} = 30, \quad \boldsymbol{r}_{01} = [0.0\ 30.0\ 50.0]^{\mathrm{T}};$$

$$\phi_{02} = \pi, \quad \varphi_{02} = 3\pi/4, \quad \boldsymbol{r}_{02} = [0.0\ -21.2132\ 21.2132]^{\mathrm{T}};$$

$$\phi_{03} = -\pi/2, \quad \varphi_{03} = -40, \quad \boldsymbol{r}_{03} = [0.0\ -50.0\ -40.0]^{\mathrm{T}}.$$

The contact regions are formulated as

$$R_i = \{\boldsymbol{r}_i \in S_i |\ \ \|\boldsymbol{r}_i - \boldsymbol{r}_{0i}\| \leqslant \rho\} \text{ for } i = 1, 2, 3.$$

Running Algorithm 1 with $\kappa = 1$ and $\rho = 0$ yields $\zeta^* = -1.4525 \times 10^{-1} < 0$, which means the grasp $\boldsymbol{G}_0$ is force-closure. Using $\rho = 3$ and running Algorithm 1 again, we get $\zeta^* = 1.4032 \times 10^{-1} > 0$; thus $\boldsymbol{G}_0$ is not force-closure with the radius $\rho = 3$. A non-force-closure grasp is found with the CPU time of 1.52 s:

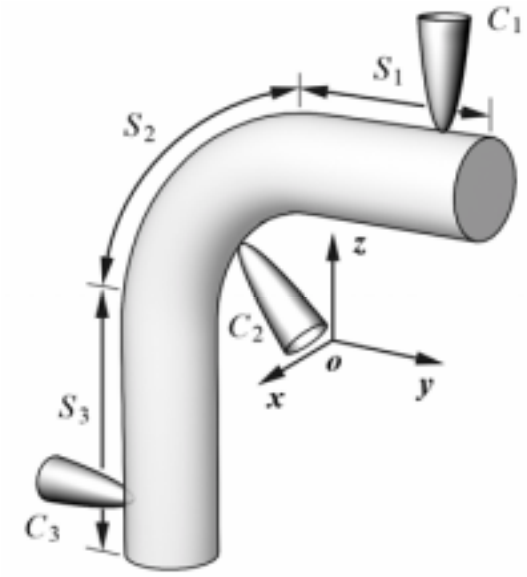

Fig. 11. An L-shaped pipe is grasped by a three-fingered gripper with point contacts with friction C_1, C_2, and C_3.

$$\phi_1^* = 1.8675, \quad \varphi_1^* = 30.5122,$$

$$\boldsymbol{r}_1^* = [-2.9235\ 30.5122\ 49.5631]^{\mathrm{T}};$$

$$\phi_2^* = 2.8405, \quad \varphi_2^* = 2.3573,$$

$$\boldsymbol{r}_2^* = [2.9659\ -21.5549\ 21.5078]^{\mathrm{T}};$$

$$\phi_3^* = -1.8656, \quad \varphi_3^* = -40.6085,$$

$$\boldsymbol{r}_3^* = [-2.9058\ -49.5685\ -40.6085]^{\mathrm{T}}.$$

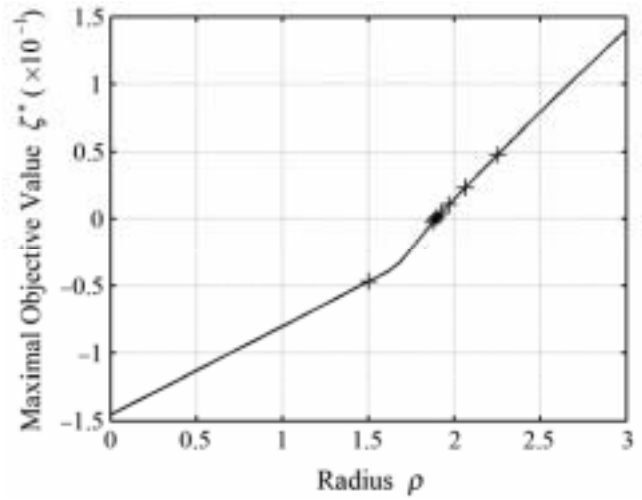

Fig. 12. The $\zeta^* - \rho$ curve obtained by Algorithm 1 when $\kappa = 1$. The plus signs indicate the data (ρ, ζ^*) in running Algorithm 2.

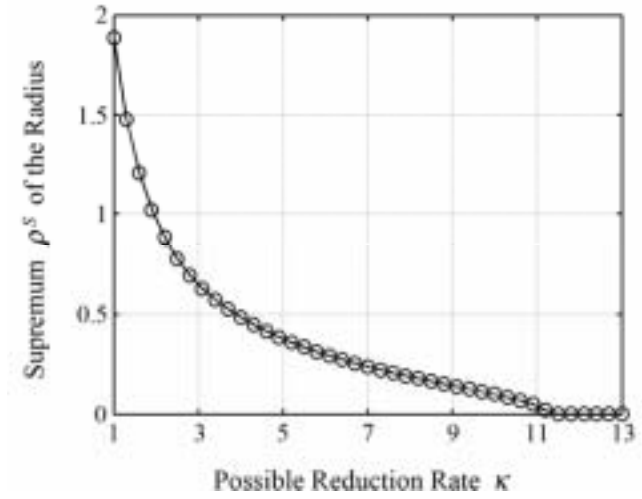

Fig. 13. The $\rho^S - \kappa$ curve for $\boldsymbol{G}_0$ obtained by Algorithm 3.

$\boldsymbol{u}^* = [9.9371 \quad -0.5496 \quad -0.4416 \quad 0.0267 \quad -0.5870 \quad -0.6413]^{\mathrm{T}} \times 10^{-1}$ is a direction of consistent infinitesimal motions of the pipe. Figure 12 describes the $\zeta^* - \rho$ curve with respect to $\kappa = 1$ and the values (ρ, ζ^*) in each loop of Algorithm 2 using $\rho^U = 3$ and $\varepsilon_\rho = 10^{-4}$. As displayed in Table 2, Algorithm 2 terminates at $\rho_1 = 1.8879$ and $\rho_2 = 1.8880$. Then $\rho^S = 1.8880$, for which $-0.0001 \times 10^{-1} < \zeta^* < 0$. The required CPU time is 24.81 s. Figure 13 shows the result of Algorithm 3. As κ increases to 13, ρ^S decreases to 0; hence the grasp $\boldsymbol{G}_0$ is not form-closure.

7. Conclusions

The existing literature on the closure properties has been summarized and classified distinctively. Although it is so extensive, no one has studied friction uncertainty and contact position uncertainty, which are the main dangers to force-closure. This paper seeks to fill this void. The former uncertainty is quantified by the possible reduction rate κ of friction coefficients, while the latter is measured by the radius ρ of contact regions. The force-closure test with given κ and ρ, the supremum ρ^S of ρ without loss of force-closure, and the $\rho^S - \kappa$ curve are three emergent problems in this respect. The first problem is solved by searching for a non-zero consistent infinitesimal motion using nonlinear programming technique (Algorithm 1). The second problem is transformed to an algebraic equation of one variable, to which the bisection method is applied (Algorithm 2). Using the two algorithms, the last problem is readily settled and its result evaluates the overall tolerance of a grasp to both uncertainties (Algorithm 3).

In order to solve the above problems efficiently, we generalize the infinitesimal motion approach from form-closure to force-closure analysis. This approach covers the three contact types, does not use linearization, and does not need to compute the rank and the null space of the grasp matrix. In the force-closure analysis, the sets of feasible contact forces, feasible resultant wrenches, consistent infinitesimal motions, and consistent functional movements are formulated. They are convex cones and are discussed systemically. In virtue of the duality between them (Figures 5 and 6), we prove that a grasp is force-closure if and only if any non-zero infinitesimal motion is inconsistent. Furthermore, an approach to computing the polar set of a compact convex set containing the origin as an interior point is addressed with application to computing the set of consistent functional movements. On this basis, looking for a non-zero consistent infinitesimal motion is formulated as a nonlinear programming problem.

Appendix: Computing the Polar Set of a Compact Convex Set Containing the Origin as an Interior Point

The set $\{\boldsymbol{x}_i\}$ is a compact convex set containing the origin as an interior point. The set $\{\boldsymbol{y}_i\}$ defined by (31) is the polar set of $\{\boldsymbol{x}_i\}$. The computation of $\{\boldsymbol{y}_i\}$ is preceded by the following lemmas.

LEMMA 2. $\{\boldsymbol{y}_i\}$ is a non-empty compact convex set containing the origin as an interior point.

Proof. It follows from that $\{\boldsymbol{x}_i\}$ is a non-empty compact convex set and contains the origin as an interior point (see Lay 1982, p. 142). □

Lemma 2 allows us to find the boundary of $\{\boldsymbol{y}_i\}$, and then $\{\boldsymbol{y}_i\}$ is the convex hull of its boundary. Let $bd\ \{\boldsymbol{x}_i\}$ and $bd\ \{\boldsymbol{y}_i\}$

Table 2. Data During the Iteration by Bisection in Running Algorithm 2 for Example 2

Loop	ρ_1	ρ_2	$\rho = (\rho_1 + \rho_2)/2$	$\zeta^*(10^{-1})$
1	0	3	1.5000	–0.4673
2	1.5000	3	2.2500	0.4778
3	1.5000	2.2500	1.8750	–0.0214
4	1.8750	2.2500	2.0625	0.2344
5	1.8750	2.0625	1.9688	0.1096
6	1.8750	1.9688	1.9219	0.0463
7	1.8750	1.9219	1.8984	0.0144
8	1.8750	1.8984	1.8867	–0.0020
9	1.8867	1.8984	1.8926	0.0063
10	1.8867	1.8926	1.8896	0.0023
11	1.8867	1.8896	1.8882	0.0003
12	1.8867	1.8882	1.8875	–0.0008
13	1.8875	1.8882	1.8878	–0.0003
14	1.8878	1.8882	1.8880	0.0001
15	1.8878	1.8880	1.8879	–0.0001

denote the boundaries of $\{\boldsymbol{x}_i\}$ and $\{\boldsymbol{y}_i\}$, respectively. To determine $bd\,\{\boldsymbol{y}_i\}$, we introduce the support function p of $\{\boldsymbol{x}_i\}$, which is the real-valued function defined by

$$p(\boldsymbol{z}) = \sup_{\boldsymbol{x}_i \in \{\boldsymbol{x}_i\}} \boldsymbol{x}_i^{\mathrm{T}} \boldsymbol{z}$$

for all $\boldsymbol{z}$ for which the supremum is finite.

LEMMA 3. If $\boldsymbol{z}$ is any fixed point other than the origin, the following hold (see Lay 1982, p. 206):

1. $\boldsymbol{x}_i^{\mathrm{T}} \boldsymbol{z} \leqslant p(\boldsymbol{z})$ for all $\boldsymbol{x}_i \in \{\boldsymbol{x}_i\}$;
2. There exists a point $\boldsymbol{x}_{bi} \in bd\,\{\boldsymbol{x}_i\}$ such that $p(\boldsymbol{z}) = \boldsymbol{x}_{bi}^{\mathrm{T}} \boldsymbol{z}$;
3. The hyperplane $H_i = \left\{\boldsymbol{x}_i |\ \boldsymbol{x}_i^{\mathrm{T}} \boldsymbol{z} = p(\boldsymbol{z})\right\}$ supports $\{\boldsymbol{x}_i\}$ at $\boldsymbol{x}_{bi}$;
4. The function is positively homogeneous: $p(\lambda \boldsymbol{z}) = \lambda p(\boldsymbol{z})$ for $\lambda > 0$;
5. $p(\boldsymbol{z}) > 0$.

LEMMA 4. If $\boldsymbol{z}$ is any fixed point other than the origin, the following hold:

1. $p(\boldsymbol{z})^{-1} \boldsymbol{z} \in bd\,\{\boldsymbol{y}_i\}$;
2. $p(\lambda \boldsymbol{z})^{-1} \lambda \boldsymbol{z} = p(\boldsymbol{z})^{-1} \boldsymbol{z}$ for $\lambda > 0$.

Proof.

1. From Lemma 3, points (1) and (5), $\boldsymbol{x}_i^{\mathrm{T}} p(\boldsymbol{z})^{-1} \boldsymbol{z} \leqslant 1$ for all $\boldsymbol{x}_i \in \{\boldsymbol{x}_i\}$. Then from eq. (31), $p(\boldsymbol{z})^{-1} \boldsymbol{z} \in \{\boldsymbol{y}_i\}$. Suppose that there is a closed ball $S(r,\, p(\boldsymbol{z})^{-1} \boldsymbol{z})$ with center $p(\boldsymbol{z})^{-1} \boldsymbol{z}$ and radius $r > 0$. Let $\boldsymbol{y} = p(\boldsymbol{z})^{-1} \boldsymbol{z} + r\boldsymbol{z} \big/ \|\boldsymbol{z}\|$. Obviously, $\boldsymbol{y} \in S(r,\, p(\boldsymbol{z})^{-1} \boldsymbol{z})$. However, from Lemma 3, points (2) and (5), $\boldsymbol{x}_{bi}^{\mathrm{T}} \boldsymbol{y} = \boldsymbol{x}_{bi}^{\mathrm{T}} p(\boldsymbol{z})^{-1} \boldsymbol{z} + r \boldsymbol{x}_{bi}^{\mathrm{T}} \boldsymbol{z} = 1 + r p(\boldsymbol{z}) \big/ \|\boldsymbol{z}\| > 1$, which means $\boldsymbol{y} \notin \{\boldsymbol{y}_i\}$. Hence $p(\boldsymbol{z})^{-1} \boldsymbol{z} \in bd\,\{\boldsymbol{y}_i\}$.
2. If $\lambda > 0$, then from Lemma 3, point (4), we readily have $p(\lambda \boldsymbol{z})^{-1} \lambda \boldsymbol{z} = \lambda^{-1} p(\boldsymbol{z})^{-1} \lambda \boldsymbol{z} = p(\boldsymbol{z})^{-1} \boldsymbol{z}$.

□

Lemma 4, point (2), implies that $p(\boldsymbol{z})^{-1} \boldsymbol{z}$ is decided only by the direction of $\boldsymbol{z}$. Then, from Lemma 4, point (1), the boundary of $\{\boldsymbol{y}_i\}$ can be expressed by

$$bd\,\{\boldsymbol{y}_i\} = \left\{ \boldsymbol{y}_i = p(\boldsymbol{z})^{-1} \boldsymbol{z} \middle|\ p(\boldsymbol{z}) = \sup_{\boldsymbol{x}_i \in \{\boldsymbol{x}_i\}} \boldsymbol{x}_i^{\mathrm{T}} \boldsymbol{z},\ \ \|\boldsymbol{z}\| = 1 \right\}.$$

From Lemma 3, points (2) and (3), $bd\,\{\boldsymbol{y}_i\}$ can be rewritten as

$$bd\,\{\boldsymbol{y}_i\} = \left\{ \boldsymbol{y}_i = (\boldsymbol{x}_{bi}^{\mathrm{T}} \boldsymbol{z})^{-1} \boldsymbol{z} \middle|\ \boldsymbol{x}_{bi} \in bd\,\{\boldsymbol{x}_i\},\ \boldsymbol{z} \in \{\boldsymbol{z}\}_{bi} \right\}$$

where $\{\boldsymbol{z}\}_{bi}$ consists of the unit outward normal vectors of all hyperplanes supporting $\{\boldsymbol{x}_i\}$ at $\boldsymbol{x}_{bi}$.

Acknowledgments

The authors are very grateful to the reviewers and the editor for their careful review and very helpful comments on the first submission of this paper. Sincere thanks also go to Dr Bing-Ran Zuo for suggesting this research topic. This work was supported by the National Natural Science Foundation of China under Grant 59685004.

References

Abel, J. M., Holzmann, W., and McCarthy, J. M. 1985. On grasping planar objects with two articulated fingers. *IEEE Journal of Robotics and Automation* 1(4):211–214.

Barber, J., Volz, A., Desai, R., Rubinfeld, R., Schipper, B., and Wolter, J. 1987. Automatic evaluation of two-fingered grips. *IEEE Journal of Robotics and Automation* 3(4):356–361.

Bekey, G. A., Liu, H., Tomovic, R., and Karplus, W. 1993. Knowledge-based control of grasping in robot hands using heuristics from human motor skills. *IEEE Transactions on Robotics and Automation* 9(6):709–721.

Bicchi, A. 1995. On the closure properties of robotic grasping. *International Journal of Robotics Research* 14(4):319–334.

Buss, M., Hashimoto, H., and Moore, J. B. 1996. Dextrous hand grasping force optimization. *IEEE Transactions on Robotics and Automation* 12(3):406–417.

Cheah, C. C., Han, H. Y., Sawamura, S., and Arimoto, S. 1998. Grasping and position control for multi-fingered robot hands with uncertain Jacobian matrices. *Proceedings of the IEEE International Conference on Robotics and Automation (ICRA)*, Leuven, Belgium, pp. 2403–2408.

Chen, I-M. and Burdick, J. W. 1993a. A qualitative test for N-finger force closure grasps on planar objects with applications to manipulation and finger gaits. *Proc. IEEE Int. Conf. on Robotics and Automation*, pp. 814–820.

Chen, I-M. and Burdick, J. W. 1993b. Finding antipodal point grasps on irregular shaped objects. *IEEE Transactions on Robotics and Automation* 9(4):507–512.

Chen, Y-C., Walker, I. D., and Cheatham, J. B. 1995. Visualization of force-closure grasps for objects through contact force decomposition. *International Journal of Robotics Research* 14(1):37–75.

Ding, D., Liu, Y-H., and Wang, S. G. 2001. Computation of 3D form-closure grasps. *IEEE Transactions on Robotics and Automation* 17(4):515–522.

Ding, D., Liu, Y-H., Wang, Y., and Wang, S. G. 2001. Automatic selection of fixturing surfaces and fixturing points for polyhedral workpieces. *IEEE Transactions on Robotics and Automation* 17(6):833–841.

Ferrari, C. and Canny, J. 1992. Planning optimal grasps. *Proceedings of the IEEE International Conference on Robotics and Automation (ICRA)*, Nice, France, pp. 2290–2295.

Han, L., Trinkle, J. C., and Li, Z. X. 2000. Grasp analysis as linear matrix inequality problems. *IEEE Transactions on Robotics and Automation* 16(6):663–674.

Howe, R. D., Kao, I., and Cutkosky, M. R. 1988. The sliding of robot fingers under combined torsion and shear loading. *Proceedings of the IEEE International Conference on Robotics and Automation (ICRA)*, Philadelphia, PA, pp. 103–105.

Lakshminarayana, K. 1978. Mechanics of form closure, Paper No. 78-DET-32, ASME, New York, pp. 2–8.

Lay, S. R. 1982. *Convex Sets and their Applications*. Wiley, New York.

Li, Z. and Sastry, S. 1988. Task-oriented optimal grasping by multifingered robot hands. *IEEE Journal of Robotics and Automation* 4(1):32–44.

Li, J-W., Liu, H., and Cai, H-G., 2003. On computing three-finger force-closure grasps of 2D and 3D objects. *IEEE Transactions on Robotics and Automation* 19(1):155–161.

Liu, Y-H. 1999. Qualitative test and force optimization of 3-D frictional form-closure grasps using linear programming. *IEEE Transactions on Robotics and Automation* 15(1):163–173.

Liu, Y-H. 2000. Computing n-finger form-closure grasps on polygonal objects. *International Journal of Robotics Research* 19(2):149–158.

Markenscoff, X. and Papadimitriou, C. H. 1989. Optimum grip of a polygon. *International Journal of Robotics Research* 8(2):17–29.

Markenscoff, X., Ni, L., and Papadimitriou, C. H. 1990. The geometry of grasping. *International Journal of Robotics Research* 9(1):61–74.

Mirtich, B. and Canny, J. 1994. Easily computable optimum grasps in 2D and 3D. *Proceedings of the IEEE International Conference on Robotics and Automation (ICRA)*, San Diego, CA, pp. 739–747.

Mishra, B., Schwarz, J. T., and Sharir, M. 1987. On the existence and synthesis of multifingered positive grips. *Algorithmica* 2(4):541–558.

Murray, R. M., Li, Z. X., and Sastry, S. S. 1994. *A Mathematical Introduction to Robotic Manipulation*. CRC Press, Boca Raton, FL.

Nakamura, Y., Nagai, K., and Yoshikawa, T. 1989. Dynamics and stability in coordination of multiple robotic mechanisms. *International Journal of Robotics Research* 8(2):44–61.

Nguyen, V. D. 1986. The synthesis of stable force-closure grasps. Technical Report No. 905. MIT A. I. Laboratory, Cambridge, MA.

Nguyen, V. D. 1988. Constructing force-closure grasps. *International Journal of Robotics Research* 7(3):3–16.

Pai, D. K. and Leu, M. C. 1991. Uncertainty and compliance of robot manipulators with applications to task feasibility. *International Journal of Robotics Research* 10(3):200–213.

Park, Y. C. and Starr, G. P. 1992. Grasp synthesis of polygonal objects using a three-fingered robot hand. *International Journal of Robotics Research* 11(3):163–184.

Ponce, J. and Faverjon, B. 1995. On computing three-fingered force-closure grasps of polygonal objects. *IEEE Transactions on Robotics and Automation* 11(6):868–881.

Ponce, J., Stam, D., and Faverjon, B. 1993. On computing two-fingered force-closure grasps of curved 2D objects. *International Journal of Robotics Research* 12(3):263–273.

Ponce, J., Sullivan, S., Sudsang, A., Boissonnat, J.-D.,

and Merlet, J.-P. 1997. On computing four-fingered equilibrium and force-closure grasps of polyhedral objects. *International Journal of Robotics Research* 16(1):11–35.

Qian, W-H., Qiao, H., and Tso, S. K. 2001. Synthesizing two-fingered grippers for positioning and identifying objects. *IEEE Transactions on Systems, Man, and Cybernetics B* 31(4):602–615.

Reuleaux, F. 1875. *Kinematics of Machinery* (first published in German). Reprinted 1963 by Dover, New York.

Salisbury, J. K. and Roth, B. 1983. Kinematic and force analysis of articulated hands. *ASME Journal of Mechanism, Transmissions, Automation, and Design* 105:35–41.

Schlegl, T. and Buss, M. 1998. Hybrid closed-loop control of robotic hand regrasping. *Proceedings of the IEEE International Conference on Robotics and Automation (ICRA)*, Leuven, Belgium, pp. 3026–3031.

Somov, P. 1900. Uber Gebiete von Schraubengeschwindigkeiten eines starren Korpers bie verschiedener Zahl von Stutzflachen. *Zeitschrift Mathematik Physik* 45:245–306.

Trinkle, J. C. 1992. On the stability and instantaneous velocity of grasped frictionless objects. *IEEE Transactions on Robotics and Automation* 8(5):560–572.

Tung, C-P. and Kak, A. C. 1996. Fast construction of force-closure grasps. *IEEE Transactions on Robotics and Automation* 12(4):615–626.

Varma, V. K. and Tasch, U. 1995. A new representation for robot grasping quality measures. *Robotica* 13(3):287–295.

Yoshikawa, T. 1996. Passive and active closures by constraining mechanisms. *Proceedings of the IEEE International Conference on Robotics and Automation (ICRA)*, Minneapolis, MN, pp. 1477–1484.

Zhang, Y. R., Gao, F., Zhang, Y. D., and Gruver, W. A. 1997. Evaluating the quality of grasp configurations for dextrous hands. *Proceedings of the IEEE International Conference on Robotics and Automation (ICRA)*, Albuquerque, NM, pp. 100–105.

Zhu, X-Y. and Wang, J. 2003. Synthesis of force-closure grasps on 3D objects based on the Q distance. *IEEE Transactions on Robotics and Automation* 19(4):669–679.

Zuo, B-R. and Qian, W-H. 1998. A force-closure test for soft multi-fingered grasps. *Science in China, Series E* 41(1):62–69.